Source processes of the M 6 class earthquakes which occurred in northern Ibaraki Prefecture on 2011 and 2016

*Kazuhito Hikima[1]

1. Tokyo Electric Power Company Holdings, Inc.

<INTRODUCTION>
An M 6.3 earthquake occurred at 21:38 on December 28, 2016 in northern Ibaraki Prefecture. Since just after the 2011 off the Pacific coast of Tohoku Earthquake(M9.0), a significant increase in the shallow normal fault type seismicity, which had been extremely rare before the 2011 Tohoku earthquake, has been observed. Furthermore, the M 6.1 earthquake had occurred on March 19, 2011, within the area. According to the analyses of InSAR data, the crustal deformations of the 2016 and the 2011 earthquakes are observed in almost same area (GSI, 2017), so, it suggests that comparable size earthquakes have repeated in the interval of only about 5.7 years.
In addition, strong ground motions, those peak accelerations are about 1G, have been recorded during both earthquakes at the KiK-net station (IBRH13, Takahagi), therefore, those records are important to consider the ground motion level at the near faults. To consider these issues, the source process inversion analyses for the 2016 and the 2011 earthquakes are performed in this study.
<OUTLINE of ANALYSES>
The 16 stations of the K-NET and KiK-net (NIED) were used in these inversion analyses. Basically, identical stations were selected for the 2016 and the 2011 earthquakes. The acceleration waveforms were filtered between 0.03 and 0.8 Hz, and were integrated to velocity waveforms for the inversion analyses.
The source processes were inverted by the multi time window analysis (Yoshida et al., 1996, Hikima, 2012). The Green’ s functions were calculated using 1-D velocity models, which were tuned by the waveform inversion method using the records of a small event (Hikima and Koketsu, 2005).
The fault planes for the initial models were configured by referring to the F-net mechanism solutions and distribution of the aftershocks, those were relocated using DD method (Waldhauser and Ellsworth, 2000). The parameters of the final models were determined by considering the degree of fitness between the observed and synthetic waveforms. The size of subfaults for the inversion analyses were set in 1 km.
<RESULT: 2016's earthquake>
The fault parameters are given as follows: the strike and the dip are 164 and 50 degree, and the length and width are 17 and 12 km, respectively. The focal depth is 10.3 km. The inversion result shows that the seismic moment is 9.7e17 Nm (Mw 5.9), and the maximum slip is about 0.7 m and the dominant focal mechanism is the normal fault type. The rupture propagated toward the northern shallow part mainly, and a large slip area (asperity) exists at 6 - 7 km apart from the hypocenter.
<RESULT: 2011's earthquake>
The fault parameters are set as follows: the strike and the dip are 141 and 40 degree, and the length and width are 15 and 11 km, respectively. The depth of hypocenter is 5.9 km. Dominant focal mechanism is normal fault type, and the estimated seismic moment is 7.0e17 Nm (Mw 5.8). The maximum slip is about 0.6 m and it is located near the hypocenter. The asperity covers the hypocenter and its slightly northern part. The amount of final slip on southern part of the fault plane is small.
<DISCUSSION>
The epicenter of the 2016's event is located at about 7 km south of the 2011's event. Though, it was revealed that the rupture of the 2016's event propagated toward the north and its asperity stands fairly near an asperity of the 2011's event. However, the strike and the dip of these events are different and it means that the fault planes of the events are not identical. Furthermore, the estimated slip distributions

show that the asperities of two events scarcely overlap each other. According to these results, it is deduced that the dominant slip areas of the 2016's and the 2011's events are different.
The KiK-net station (IBRH13), at which high accelerations were observed, is located adjacent to the asperities of these events. Especially, the asperity of 2011's event was recovered just below the IBRH13. The PGA of the 2011's and 2016's events was 1084 gal and 887 gal, respectively (3 components synthesized, from NIED's HP). This higher PGA of the 2011's event, although the magnitude is smaller than the 2016's event, is thought to be due to its closer distance from the asperity.

Keywords: Source process, Crustal earthquake, Strong motion, Repeating earthquake, Northern Ibaraki Prefecture earthquake

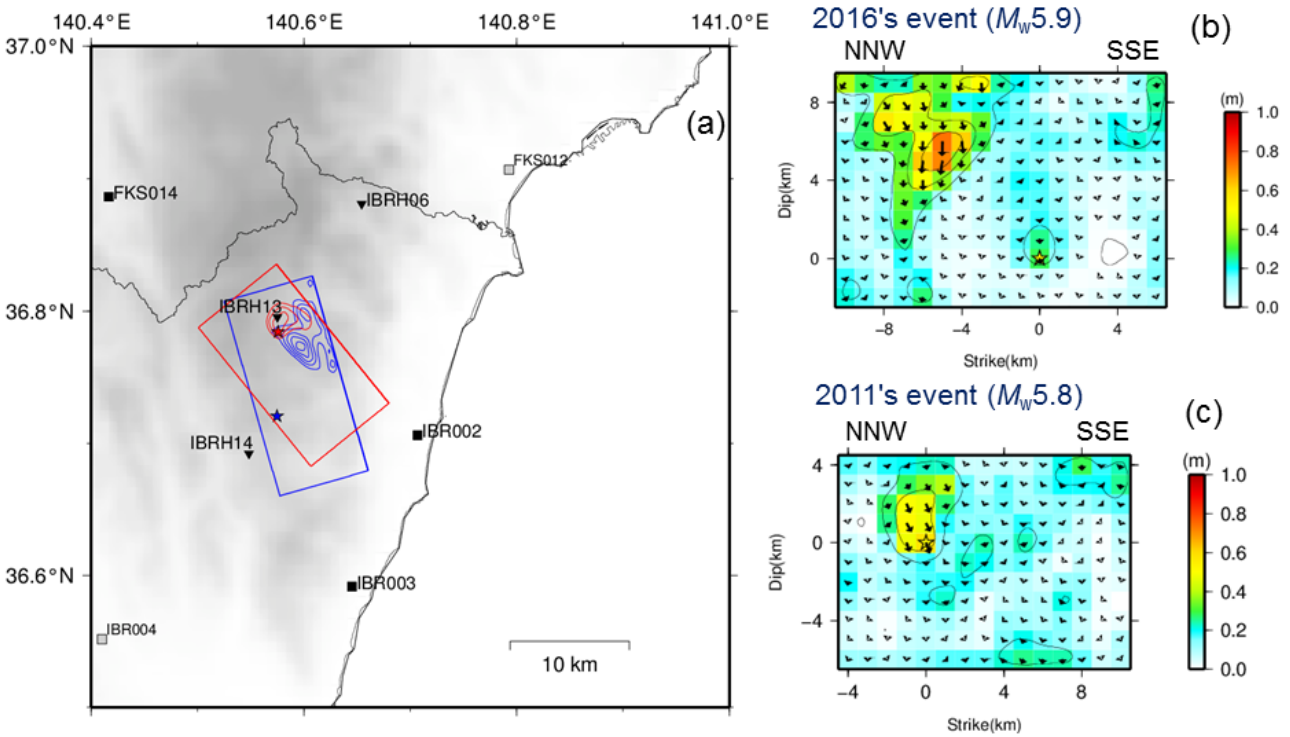

(a): Surface projection of the final slip distribution of 2016's and 2011's events. Blue denotes the 2016's event and red denotes the 2011's event. Squares and stars indicate set fault planes and epicenters, respectively. Contour shows slip area larger than 0.3 m, with interval of 0.1 m. Black marks denote KiK-net and K-NET stations.
(b), (c): Final slip distributions on fault planes of 2016's and 2011's events. The yellow stars mean hypocenters.

Estimation of the source location of the 16-April-2016 Oita induced earthquake with array analysis

Kenta Doihara[1], *Masanao Komatsu[2], Hiroshi Takenaka[2]

1. Department of Earth Sciences, Okayama University, 2. Graduate School of Natural Science and Technology, Okayama University

At the 14 April 2016, the mainshock of the 2016 Kumamoto earthquakes (M_{JMA} 7.3) occurred in Kumamoto Prefecture. After about 32 seconds from the origin, the induced event took place in Yufu, Oita prefecture. Looking on the seismograms, high-frequency phase is found following the phase of the mainshock, and can be clearly seen in the stations near the hypocenter. JMA determined the hypocenter of induced event by mainly picking S-wave arrival. Since phases of this event were contaminated due to the mainshock, the number of picked P-wave arrival was only four stations. Yoshida (2016) and Miyazawa (2016) also determined the hypocenter by picking out P- and S-wave arrivals in stations near the hypocenter. Nakamura and Aoi (2017) estimated the hypocenter location by the back-projection method using an acceleration envelope. In this study, we determine the source location using a horizontal slowness and an azimuth estimated by semblance method as a kind of array analysis. This method is employed for S phases observed in surround of the source region and a distance from there. We used the seismograms observed in K-NET, KiK-net and F-net of NIED, and seismic intensity stations of JMA and Oita prefecture. We set 5 arrays constructed each 3 stations. In the result of hypocenter determination using the azimuth and the slowness estimated in each arrays, the source location is 33.277N, 131.420E, 10.7 km depth. Seen from the hypocenter determined by JMA, the position by this study is off from the east side. Calculating PGA and PGV in 5 stations near the source, OIT009 in K-NET has higher PGA than other stations and highest PGV, where high site-amplification is modeled in Yufu basin. Although site-amplification is lower than OIT009, Tsurumi intensity station in JMA has largest PGA. These features denote that the source location might be located in the position of eastern side of the JMA’ s location. Moreover we estimate moment magnitude using a flat level of S-wave displacement spectrum in 2 stations near the source. Modifying the site effect using observed spectrum in maximum aftershock (M_{JMA}5.4), we obtained M_w 5.5. Also, since the aftershocks did not hardly occur in surround the source location estimated by this study, we think that this area is the asperity of the induced event.
Acknowledgements: This work is partially supported by the Comprehensive Research on the Beppu-Haneyama Fault Zone funded by the Ministry of Education, Culture, Sports, Science, and Technology (MEXT), Japan. We use strong motion records of NIED, JMA and Oita prefecture.

Keywords: Oita induced earthquake, Semblance method, Array analysis

On Application of Dynamic Rupture Simulations to Assess Possible Earthquake Source Parameters for Beppu-Haneyama Fault Zone, southwestern Japan

*Ryosuke Ando[1], Kazutoshi Imanishi[2], Hiroe Miyake[4], Masayuki Yoshimi[2], Shinichi Matsushima[3]

1. Graduate School of Science, University of Tokyo, 2. National Institute of Advanced Industrial Science and Technology, 3. Disaster Prevention Research Institute, Kyoto University, 4. Earthquake Research Institute, University of Tokyo

For the strong ground motion prediction, increasing the physical constraints for source models is important to increase the predictability of the phenomena caused by possible future earthquakes. Currently standard approaches constrain the source models basically with the macroscopic characteristics of the slip-fault length scaling in a kinematic manner, where fault lengths, faulting styles and slip distributions are determined based on judgements of professionals. Relaying on such external information causes major difficulties of this approach since it contains large ambiguities due to observational limitations and, further, it is not necessarily physically based.
In this study we aim to utilize results of dynamic rupture simulations to provide the constraints of the source parameters targeting hypothetical future earthquakes generated along the Beppu-Haneyama fault zone (BHF), which exists as western continuation of the median tectonic line, southwestern Japan. The western part of BHF had been broken during the 2016 Kumamoto earthquake sequence. We constrained our dynamic model based on the regional stress field obtained basically by the seismological stress tensor inversions (Matsumoto et al., 2015) and newly modified fault geometry there, consisting of the three segments called the Funai-Asamigawa-Hotta (hereafter Funai), the Misa and the Hoyo channel from the west. The nonplanar geometry of these fault segments is treated by the spatio-temporal boundary integral equation method (ST-BIEM) with the fast domain partitioning method. The simulation results show, for example, the rake angles differ by up to approximately 30 degrees from the values assumed based on the recipe for kinematically predicting strong motion, namely 90 degrees for the Funai and Misa segments and the 180 degrees for the Hoyo channel segment. The dynamic rupture simulations may provide additional information for the strong ground motion prediction regarding the rupture/slip profiles, which are physical and natural outcome of the model.
This work is supported by the Comprehensive Research on the Beppu-Haneyama Fault Zone funded by the Ministry of Education, Culture, Sports, Science, and Technology (MEXT), Japan.

Keywords: Beppu-Haneyama fault zone, Dynamic earthquake rupture models, Boundary integral equation method

Source, path, and site effects of intraslab and interplate earthquakes off Miyagi Prefecture in Northeastern Japan

*Yasumaro Kakehi[1]

1. Department of Planetology, Graduate School of Science, Kobe University

Kasatani and Kakehi (2014) made spectral inversion analysis of the intraslab and interplate earthquakes off Miyagi Prefecture in Northeastern Japan using K-NET strong ground motion data of NIED. Their result showed that the high-frequency levels of intraslab and interplate earthquakes with nearly the same depth are nearly the same, and that the high-frequency level depends simply on source depth and is higher for deeper source, independent of tectonic environments such as intraslab and interplate earthquakes. In previous studies, the view that high-frequency level of intraslab earthquake is higher than that of interplate earthquake has been widely accepted. On the other hand, some studies (e.g. Kato et al. (1999)) presented another view that high-frequency level depends simply on source depth, independent of tectonic environments, and high-frequency level is higher for deeper source. Result of Kasatani and Kakehi (2014) supported the latter.
Kakehi (2016) selected three events with different depths, whose epicenters are aligned linearly, from the events that Kasatani and Kakehi (2014) studied, and made an analysis of attenuation relation of peak ground acceleration using NIED K-NET and KiK-net strong ground motion data. He showed that the slope of the decay of attenuation relation of the deepest event is obviously steeper than those of the other two shallow events. This kind of depth-dependent trend of attenuation relation is frequently seen in previous studies.
In the spectral inversion of Kasatani and Kakehi (2014), common attenuation relation is assumed for all the events, independent of source depths. In this case, attenuation relation that is actually depth-dependent is attributed to source and site effects. Actually, the attenuation relations of the acceleration amplitudes with the site effects (obtained in the spectral inversion) removed shows similar gentle slope of decay for all of the three events. This means that in the spectral inversion of Kasatani and Kakehi (2014), the strength of attenuation is underestimated for deeper events, and therefore, the high-frequency level of source effect is also underestimated for deeper events.
When this underestimation of high-frequency level of deeper source is considered, high-frequency levels of deeper events will be higher than those obtained in Kasatani and Kakehi (2014). That is, validity of the conclusion itself that high-frequency level is higher for deeper source by Kasatani and Kakehi (2014) is supported, and the depth dependency of high-frequency level is more enhanced.
In the presentation, detailed report on source, path, and site effects of the intraslab and interplate earthquakes off Miyagi Prefecture is given, based on the evaluation of site effects from the inversion of "network of adjacent two station pairs" by Ikeura and Kato (2011) that does not assume attenuation functions.

Keywords: high-frequency level, intraslab earthquake, interplate earthquake, focal depth, attenuation relation, site effect

Analysis of Systematic Path Effects form Ground-Motion Variability Using Different Path-Bin Plans

*CHIH HSUAN SUNG[1], Chyi-Tyi Lee[1]

1. National Central University-Graduate Institude of Applied Geology

This paper describes the path diagram method should aim to the record-to-record residuals of a single earthquake instead of a single station, to solve the limitations of the bracket. We use 150 shallow earthquakes with moment magnitudes greater than 4.0 obtained from the Taiwan Strong-Motion Instrumentation Program network to build the Taiwan ground-motion prediction equations for peak ground acceleration and spectral accelerations with 5% damping for different structural periods. The record-to-record residuals are divided into small brackets in a path diagram for six distance bins and twenty-four azimuth bins. The mean residuals are estimated for each path bin, from which we can get 144 inter-path residuals for a source and compute a repeatable path-term for all inter-path residuals. Comparing the results with those obtained with the same data, but using the path diagram of a site, show that we obtain a lower remaining variance and the higher repeatable path-term with the 15˚ bracket of the path diagram approach for a source. The remaining unexplained intra-event standard deviations are 40-44% smaller than the record-to-record standard deviation for peak ground acceleration and spectral accelerations at periods of 0.3, 1.0, and 3.0 seconds. The results of path-to-path variability of each earthquake show that some earthquakes of small magnitude have a higher sigma because their source-to-site distances almost locate in the range of 0-50 km.

Keywords: GMPE, aleatory variability, strong ground motion, path effect, PSHA

The single-path standard deviation derived from ground motion records in Japan

*Tomoki Hikita[1], Kazuki Koketsu[2], Hiroe Miyake[3]

1. Kajima Corporation, 2. Earthquake Research Institute, University of Tokyo, 3. Center for Integrated Disaster Information Research, Interfaculty Initiative in Information Studies, University of Tokyo

1. Introduction
The amplitude of a ground motion record includes aleatoric variability, even if the records observed at one site by the earthquakes with same magnitude and same location. It is important to clarify the characteristics of such variability in order to understand the accuracy of earthquake ground motion prediction. Using ground motion records from dense networks, several recent studies (e.g. Anderson and Uchiyama, 2011; Lin et al., 2011) have estimated the single-path standard deviations by removing ergodic assumption. Those studies are based on the difference between observed ground motion amplitude and a ground motion prediction model. Estimated variabilities may be affected by modeling error of applied ground motion prediction model. In this study, the single-path standard deviation have investigated directly from the amplitude ratio of pairs of ground motion records observed at one site by two earthquakes with same magnitude and same location.
2. Data and Method
The amplitude ratios of pairs of ground motion records by two earthquakes have been investigated. The two earthquakes satisfy the following conditions. 1) JMA magnitudes (M_J) are the same. 2) Focal mechanisms are similar. 3) Distance between hypocenters is 3 km or less. Pairs of ground motion records of K-NET and KiK-net by two earthquakes have been used. Hypocentral distances of records are 5 or more times of the distance between hypocenters of two earthquakes, and 200km or less. Maximum acceleration of the records at free-field exceeds 1 cm/s^2. As a result, 39,103 pairs of record by 696 pairs of earthquake were used for this study. The single-path standard deviation (*sigma*) estimated by variance of the natural logarithmic acceleration response spectrum ratio (v) of record pairs. $sigma=(Var[v]/2)^{0.5}$. The acceleration response spectrum was averaged of two horizontal components.
3. Results
Estimated *sigma* from all data was about 0.3 - 0.45 (Fig. 1). This result at period of 0.02 s was consistent with single-path standard deviations for maximum acceleration from previous studies (Morikawa et al., 2008; Lin et al., 2011). In Fig. 1, *sigma* was slightly large around the period of 0.2 s. According to comparison of *sigma* estimated from data of every magnitude range, the dominant period of *sigma* moved to the longer period depending on magnitude (Fig. 2). Since site and propagation path of each record pairs are the same respectively, the main factor of *sigma* is considered to be the differences in the source characteristics of two earthquakes. If the rupture processes of two earthquakes are different, the within-event variability of pairs of records from two earthquakes may be large around corner frequencies of two earthquakes. The dominant period of *sigma* from large earthquakes was longer than that from small earthquakes. The logarithms of the dominant period of *sigma* were proportional to about $0.4M_J$ (Fig. 3). Those characteristics of *sigma* indicate that the uncertainty of rupture process is one of the factors in single-path standard deviation.

Keywords: ground motion, response spectrum, variability, uncertainty

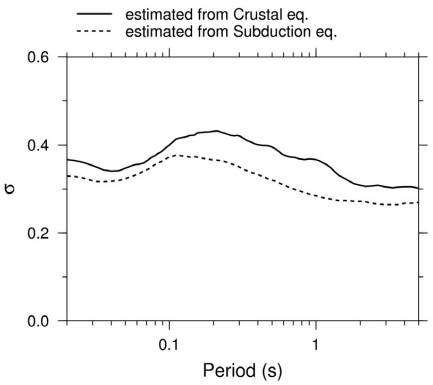

Fig. 1 Estimated single-path standard deviation σ. Solid line shows σ from data by crustal earthquakes. Dotted line shows σ from data by subduction earthquakes.

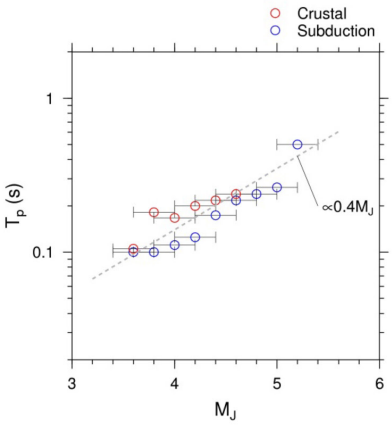

Fig. 3 Dominant period (T_p) of single-path standard deviation from data of every magnitude range. Red circle and blue circle shows T_p from data by crustal earthquakes and subduction earthquakes. Dotted line shows the approximate slope to M_J.

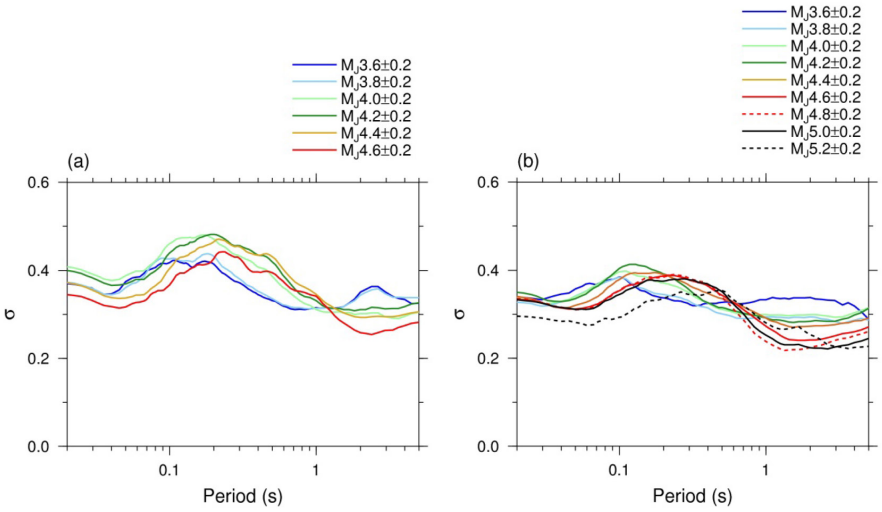

Fig. 2 Single-path standard deviation σ estimated from data of every magnitude range. (a) σ from data by crustal earthquakes. (b) σ from data by subduction earthquakes.

Attenuation characteristics of high frequency strong motions due to inland earthquakes in the Pacific coast of Tohoku region

*Tomonori Ikeura[1]

1. Kajima Technical Research Institute

In order to decrease errors of empirical strong motion prediction, the author studied detail attenuation characteristics of strong ground motions observed at K-NET and KiK-net sites in the Tohoku and Kanto regions during events occurred in Hamadori region of Fukushima Prefecture and northern Ibaraki prefecture. Attenuation characteristics of strong motions from these events were investigated using base rock motion amplitudes converted from observed ones by cancelling site amplification effect using relative site factors. These relative site factors were evaluated by Ikeura and Tomozawa(2012) so as to satisfy all relative site factors between adjacent two sites in the K-NET and KiK-net observation networks in the region using least square method without attenuation functions. In this study, attenuation characteristics of high frequency strong motions due to the 23 March 2011 and 11 April 2011 Hamadori in Fukushima prefecture earthquakes and the 19 March 2011 and 28 December 2016 northern Ibaraki prefecture earthquakes, which epicenters were arranged almost in the N15E direction, were discussed based on amplitude distributions of converted base rock motions from these events with hypocentral distances. The distributions of the amplitudes of converted base rock motions at all sites showed clear attenuation curves for these all events. Results of investigations on distributions of the converted base rock motion amplitudes at the sites in the N15E direction from epicenter of each event were as follows: (1) Base rock motion amplitudes in the north region of epicenters were larger than in the south region, indicating source characteristics of northward stronger high-frequency radiations. (2) Attenuation of converted base rock motions in the direction of N15E showed quite weak Qs effect in the distances up to 100 - 150km from epicenters. (3) Steeper attenuation was observed in the distances over 150km in the south area of epicenters than in the north area.

Keywords: strong motions, inland earthquakes, attenuation characteristics

Non-Causal Zero-Phase Filters Underpredict NGA 2 GMPE’s for Long-Period, Near-Source Motions of Large Earthquakes

*Becky Roh[1], Kenny Buyco[1], Thomas H Heaton[1]

1. California Institute of Technology

The Lucerne record from the 1992 M7.3 Landers earthquake had motions too large to be accommodated by the San Bernardino Law and Justice Center. This is problematic because this structure was designed for maximum ground motion with triple pendulum base isolators. We investigated the predictions for 10-second response spectral displacements and found that NGA 2 GMPEs under-predict, specifically long-period, near-source motions from large earthquakes. The under-prediction may be due to the conventional data processing method used in the NGA ground-motion database, which is a non-causal zero-phase Butterworth filter at a corner frequency corresponding to the expected level of noise in the record.

Theoretically, a non-causal zero-phase filtered response is approximately half the value of the response with no filter. We can see this by filtering a unit step function, in which we get a response with half the amplitude of the original, unfiltered function. While non-causal zero-phase filtering leaves the acceleration unchanged, the effect of the corner frequency in this filtering is noticeable when we integrate twice to obtain the displacement. Therefore, because long period components of the recorded ground motion may contain valuable information, it is critical to choose the appropriate period of the non-causal zero-phase filter.

We examine the strong motion data from large earthquakes, such as the 1999 M7.7 Chi-Chi, 2015 M7.8 Nepal, 2016 M7.0 Kumamoto, and 2016 M7.8 New Zealand earthquakes. We apply the baseline correction to the uncorrected acceleration records, in which we account for the linear trend in velocity. Then, we integrate for the peak displacement. The same process is applied to the acceleration records that are non-causal zero-phase filtered at 10 seconds and 60 seconds. We compare the baseline corrected displacement responses of these earthquakes to the filtered ones. Ultimately, we take these broadband ground motion records containing long period effects, conduct both linear and nonlinear response analyses of tall buildings, and observe how static offset affects these responses.

Long-period ground motion in the Kanto basin during the 2016 Kumamoto earthquake

*Tomiichi Uetake[1]

1. Seismic Design Group, R&D Department, TEPCO research Institute, Tokyo Electric Power Company

During the M 7.3 Kumamoto earthquake of April 16, 2016, the long-period ground motion was observed in the metropolitan area about 900 km from the epicenter. It is important to understand the characteristics of the seismic motion that incident to the Kanto basin and the seismic response of the basin to it for evaluation of the earthquake ground motion in the metropolitan area during a large earthquake in the western part of Japan.
First, in order to confirm the incident wave to the basin, the velocity traces of F-NET were examined from the vicinity of the epicenter to around the Kanto region. There was a remarkable wave group with the dominant period of about 10 seconds and the duration of about 60 seconds in the transverse component, and it was propagated to the Kanto basin with the apparent velocity of about 3.3 km/s. This wave group showed dispersion characteristics and is considered to be a Love wave. In addition, the waveform of the Kanto Mountains in the west side of the basin was similar to the waveform of the western part of the basin, and this group of waves is considered to be an incident wave to the basin.
Next, we examined the change of the waveform features of the observation point in the basin. Wave packets were amplified in the basin and the duration of wave packets was extended. However, the dominant period of the seismic motion was about 10 seconds at any observation point. It suggests that the influence of the incident wave is large. In addition, the amplitude of velocity response spectra at the period of 10 seconds tended to be larger toward the east side, which were about 2 cm/s at the bedrock in the west side of the basin, 5 to 10 cm/s in the western part of the basin, and 10 to 20 cm/s in the eastern part of the basin. It seems that not only the amplification by the low velocity sediment but also the extension of the duration are related to the amplification of the velocity response spectra.
The duration of the wave packet changes with the propagation of the wave packet and tends to be longer on the east side than the west side of the basin. From the multiple filter analysis of the velocity waveform, it is confirmed that the dispersion of the seismic waves influences the extension of the duration, and that the wave groups are more dispersed in the eastern observation point. The velocity waveform from Shinjuku (SNJ) to Chiba (CHB) and Togane (TGN) are shown in the figure. The duration of wave packet is about 90 seconds at Shinjuku (SNJ) in the west side, but over 180 seconds at Chiba (CHB) in the east side. The duration of the wave packet with the period of 10 seconds greatly changes in about 45 km.
Although the seismic ground motion of the north-south component was dominant in the western part of the Tokyo Bay, the large wave packets of the east-west component can be seen in the latter part of the wave traces in the east side. Examining the velocity locus shows that the dominant direction of vibration changes with the lapse of time. It suggests that the wraparound of surface waves due to the three-dimensional structure of the basin.
For this analysis, we used the records from Tokyo Electric Power Company, Japan Meteorological Agency and National Institute of Earth Science and Disaster Resilience (F-NET, K-NET, KiK-net). We used GMT for drawing figures.

Keywords: The 2016 Kumamoto earthquake, Surface wave, Long-period strong ground motion, Kanto basin

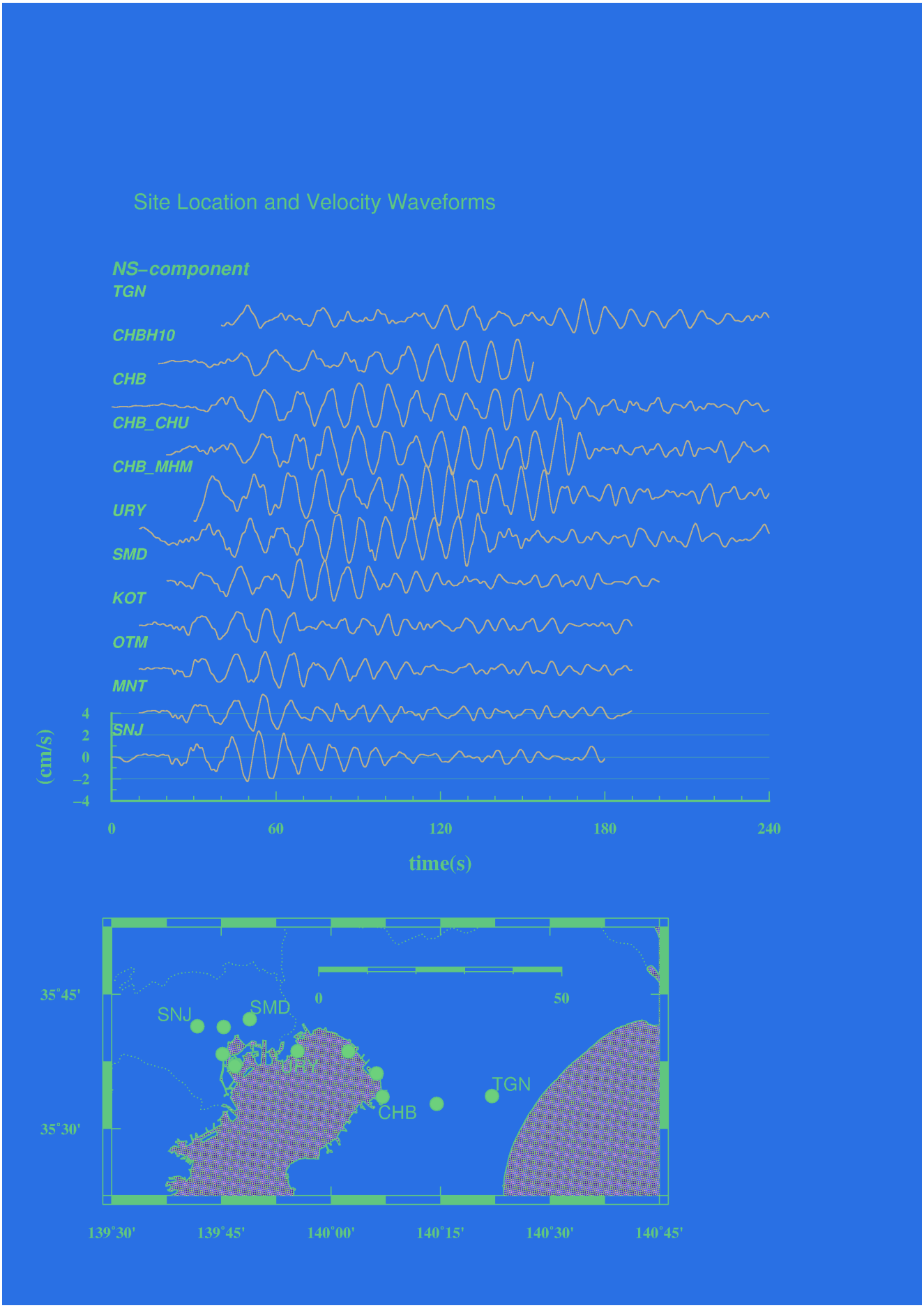

Observation and preliminary 3-D finite difference simulation of long-period ground motions (3 - 15 s) for the 2016 Mw 7.1 Kumamoto earthquake

*Yadab Prasad Dhakal[1], Shin Aoi[1], Takahiro Maeda[1], Takashi Kunugi[1], Hisahiko Kubo[1], Wataru Suzuki[1], Takeshi Kimura[1]

1. National Research Institute for Earth Science and Disaster Resilience

The Mw 7.1 Kumamoto earthquake, which occurred on 16th April, 2016, at 1:25 local time, is the largest inland earthquake to occur in Japan after the dense installation of K-NET and KiK-net strong-motion stations. Many previous studies based on the recorded ground motions from this earthquake noted that the non-existence of long-period structures such as high-rise buildings in the source area of the earthquake avoided potential risk that could be incurred due to the extremely large response spectra at periods of ~ 3 s to 7 s (e.g., Furumura, 2016). The occurrence of long-period ground motions near the source fault area of large earthquakes, particularly associated with the direct fault movement, has been well documented after the 1999 Chi Chi earthquake (Mw 7.6). On the other hand, if the size of earthquake becomes bigger such as the 1985 Mexico City earthquake (Ms 8.1), 2003 Tokachi Oki earthquake (Mw 8.3), 2011 Tohoku Oki earthquake (Mw 9.1), damaging long-period ground motions could be observed several hundred kilometers far from the source area. The 2016 Kumamoto earthquake also excited long-period ground motions at distant basins such as the Osaka basin which is located at a distance of about 400 km from the source area. Nonetheless, the motions were moderate and did not cause harmful effects on humans and infrastructures. The Kumamoto earthquake also reconfirmed that the long-period ground motions can propagate effectively in the north east region from the source area of the earthquake due to radiation pattern of the typical fault motions and crust-mantle structure in the region (Dhakal et al., 2016). In this paper, we describe the observed characteristics of long-period ground motions from the earthquake and compare a large number of recordings with synthetics from 3-D finite difference simulations. We employ the 1st grade subsurface velocity model reconstructed for the prediction of long-period ground motions by Headquarters for Earthquake Research Promotion and the source rupture model by Kubo et al. (2016) who used strong motion recordings within a distance of 100 km of the source fault for inversion. This study is expected to contribute to better understanding of the performance of the velocity and source models for the prediction of long-period ground motions from future big earthquakes.

References

Dhakal YP, Suzuki W, Kimura T, Kunugi T, Aoi S, 2016, Analysis of long-period response spectra from the 2016 Mw 7.1 Kumamoto earthquake. In proceedings of JAEE annual meeting P4-20.
Furumura T, 2016, Destructive near-fault strong ground motion from the 2016 Kumamoto prefecture, Japan, M7.3 earthquake. Landslides 13:1519-1524.
Kubo H, Suzuki W, Aoi S, Sekiguchi H, 2016, Source rupture processes of the 2016 Kumamoto, Japan, earthquakes estimated from strong motion waveforms. Earth Planets Space 68:161.

Keywords: Kumamoto earthquake, Long-period ground motions, Finite difference method

Generation conditions of long period ground motion in Kanto Basin

*Yurie Mukai[1], Takashi Furumura[1]

1. Earthquake Research Institute, The University of Tokyo

Purpose of the study

In the Kanto Basin in Japan, the long-period ground motion with period between 3 to 10 s is strongly developed when large and shallow earthquakes occur nearby Tokyo. The cause of the long-period ground motion is explained by the seismic waves generated from the shallow earthquakes, propagating over long distances, and strongly amplified in the thick sedimentary layer of the basin. The edge of the basin is considered as a secondary seismic source to develop surface wave.
Recent studies reported that the level of the long-period ground motion was very large from the earthquakes in Niigata but is weaker from the earthquakes in Tohoku (Yuasa and Nagumo, 2012; Furumura, 2014). It is considered that various causes such as the influence of the 3-D structure of the basin, the propagation path, and the orientation of the earthquake to the Kanto Basin are involved in the generation intensity of the long-period ground motion. In order to investigate the cause of the earthquake-dependent development properties of the long-period ground motion in the Kanto Basin, we examined several possible causes based on the seismic wave propagation simulation of the 2004 Niigata Prefecture (Mw6.8) Chuetsu Earthquake (hereafter denote Chuetsu Earthquake).

Orientation of earthquake and generation of long-period ground motion

In order to evaluate the influence of the orientation of the earthquake source in the long-period ground motion generation in the Kanto Basin, we carried out a 3-D finite-difference method simulation of the seismic wave propagation using a sedimentary structure model in the area around Kanto (JIVSM; Koketsu, 2012). We examined the waveform from a set of virtual source based on the fault model of the Chuetsu Earthquake which are placed at equidistance from the Kanto Basin and the direction from northeast to southeastward. The result shows that the long-period ground motion is stronger when the source locates in the direction of the Niigata Chuetsu, and is weaker of the Tohoku. However, the difference was only about 4 times with the velocity response of the natural period of 6 s, which is insufficient to explain a large difference in observation (about 10 times; Furumra, 2014).

Radiation characteristics of surface waves from a source fault

Therefore, we investigated an another cause to examine the radiation characteristics of the surface wave from the source. Here, we conducted a set of wave propagation simulation of the Chuetsu Earthquake with modifying strikes of the source fault. As a result, the level of the long-period ground motion and the peak period of the response spectrum greatly changed with change of the fault strike, which is much larger than that of the source azimuthal effect. Also, it is confirmed that the response level of the long-period ground motion at 6 s becomes largest when the fault strike corresponds to that of the Chuetsu Earthquake (212 deg.).

“Basin-Induced Surface Wave” and “Basin-Transduced Surface Wave”

As a cause of the long-period ground motion in the basin, two different mechanisms, the “Basin-Induced Surface Wave” in which the surface waves generated by conversion from the S waves at the edge of the basin and the “Basin-Transduced Surface Wave” in which the surface waves traveling to the basin is amplified to develop other surface waves, are generally discussed (for example, Kawase and Sato, 1992; Kawase, 1993). In order to investigate the contribution of the basin-induced surface waves in the Kanto

Basin during the Chuetsu Earthquake, we examined by simulation using the model where the free surface is replacing with the rigid boundary condition in the propagation path in order to prevent the propagation of the surface wave to the basin. As a result, the amplitude of the long-period ground motion in the basin drastically decreased, and the velocity response level in the period over 3 s a are weakened to about 1/2. Therefore, it is concluded that the contribution of the basin-induced surface wave is small in generating the long-period ground motion, and is mostly occurred by the surface wave traveling into the Kanto Basin.

Summary and future works

From the above discussion, the strong long-period ground motion observed in the Kanto Basin during the Chuetsu Earthquake was due to the two facts that the surface wave was radiated strongly in the Kanto direction from the source and the surface wave propagated very efficiently to the basin through the propagation path. On the other hand, for the Tohoku earthquake, the opposite situation is conceivable, i.e., the inefficient radiation of the surface wave from the source, and strong attenuation of the surface wave in the propagation path along the Pacific Ocean to the Kanto Basin.

Keywords: long-period ground motion, Kanto Basin, surface wave

Spatial distribution of ground-motion variability in broadband ground-motion simulations

*Asako Iwaki[1], Takahiro Maeda[1], Nobuyuki Morikawa[1], Hiroyuki Fujiwara[1]

1. National Research Institute for Earth Science and Disaster Resilience

Ground-motion prediction for a scenario earthquake requires evaluation of both the average ground-motion level and ground-motion variability due to model uncertainties.
This study aims to evaluate the ground-motion variability due to aleatory variability of the source parameters by modeling ground motion of the 2000 Tottori earthquake (strike-slip type) and the 2004 Chuetsu earthquake (reverse-fault type).
The source models are based on the characterized source model by the “recipe” (HERP, 2016) with fault location, size, and geometry as given parameters. Aleatory variability for the three source parameters is considered: (1) asperity location, (2) rupture initiation point, and (3) seismic moment. Two asperities are randomly located on the fault with no overlapping. A rupture initiation point is chosen randomly from the 2 km grids on the fault. Seismic moment M_0 is sampled from a normal distribution in which the mean value is given by the M_0-S relation (S being the fault area) by Irikura and Miyake (2001) and mean+2 σ equals to $2M_0$. Short-period level A, another important parameter in the characterized source model, is derived from A-M_0 relation by Dan et al. (2001).
Ground motion for each earthquake is simulated by a hybrid approach; 3D FDM (Aoi and Fujiwara, 1999) for long periods (> 1 s) and the stochastic Green’s function method (Dan and Sato, 1998) for short periods (< 1 s), using a set of 50 source models and a 3D velocity model of J-SHIS v2 (Fujiwara et al., 2012). For the 2004 Chuetsu earthquake, simulations using a simple 1D stratified velocity model are also conducted in order to exclude the effects of the complicated subsurface structure around the source area.
From the ground-motion simulation results with 50 source models for each earthquake, standard deviation (SD) of ground-motion indexes, ln of 5% damped acceleration response (Sa), PGA, and PGV, are analyzed at 10 km interval mesh. Distance and azimuthal dependence of SD are observed; the characteristics of the spatial distribution of SD differ from short periods to long periods. It is also found that the spatial distribution of SD is largely distorted by the complicated subsurface velocity structure for the Chuetsu earthquake.
As a step toward constructing a model of ground-motion variability in ground-motion prediction for a scenario earthquake, we attempt to fit the SD, each for strike-slip type and reverse-fault type, with a simple regression model using the fault distance and directivity parameters.
Effects of variability in other source parameters, such as rupture velocity and source time function, should be studied in our future works. Modeling variabilities in such source parameters requires investigation in physics- or empirical-based criteria.

Keywords: ground-motion prediction, ground-motion variability, source parameter, uncertainty

Broadband strong motion simulation for the Beppu-Haneyama Fault Zone based on the recipe

*Masayuki Yoshimi[1], Hiroe Miyake[2], Ryosuke Ando[2], Shinichi Matsushima[3], Haruhiko Suzuki[4], Shunpei Manabe[4], Hisanori Matsuyama[4]

1. Geological Survey of Japan, AIST, 2. Tokyo University, 3. DPRI, Kyoto University, 4. Oyo Corporation

We studied strong ground motions of hypothetical earthquakes along the Beppu-Haneyama Fault zone. Synthetic ground motion has been calculated with a Hybrid technique composed of a stochastic Green's function method (for HF wave), a 3D finite difference (LF wave) and 1D amplification calculation. Fault model consists of three fault planes, "Funai", "Misa", and "Hoyo strait", is employed, where the locations are determined from reflection surveys and active fault map. The rake angles are calculated with a dynamic rupture simulation considering stress filed around the faults (Ando et al, JpGU-AGU2017). Fault parameters such as the average stress drop, a size of asperity etc. are determined based on the recipe (Irikura & Miyake 2001, 2011). Three dimensional subsurface velocity structure model of Oita prefecture that was newly constructed based on the results of surveys and observations for the comprehensive research (Yoshimi et al., JpGU-AGU 2017) has been used.

This work is supported by the Comprehensive Research on the Beppu-Haneyama Fault Zone funded by the Ministry of Education, Culture, Sports, Science, and Technology (MEXT), Japan.

Keywords: strong ground motion, active fault, hybrid method, Oita

Strong Motion Simulation considering the Fault Parameters based on Dynamic Rupture Simulation on the Beppu-Haneyama Fault Zone

*Shinichi Matsushima[1], Masayuki Yoshimi[2], Ryosuke Ando[3], Hiroe Miyake[4], Haruhiko Suzuki[5]

1. Disaster Prevention Research Institute, Kyoto University, 2. Geological Survey of Japan, AIST, 3. Graduate School of Science, The University of Tokyo, 4. The University of Tokyo, 5. Oyo Corporation

As part of the comprehensive research on the Beppu-Haneyama Fault, we have been studying the dynamic rupture process on the Beppu-Haneyama Fault (Ando et al., JpGU-AGU2017). In this study, we will focus on strong motion simulation considering the fault parameters based on the parameters that were derived from the dynamic rupture simulation on the fault zone. The fault model consists of three segments of the Beppu-Haneyama Fault zone, namely “Funai, Asamigawa, Hotta (hereafter, Funai)”, “Misa”, and “Hoyo strait (hereafter, Hoyo)” segments from west to east along the southern part of the Beppu Bay. When the dip angle for Funai, Misa and Hoyo segments are assumed to be 45, 45 and 75 degrees respectively, the rake angle are calculated to be about -67, -104 and -147 degrees respectively (Ando et al, JpGU-AGU2017). Also, we consider the time delay between the segments, especially the time delay between Misa and Hoyo segments because the two segments do not overlap with each other and how the rupture propagates would rely on the dynamic conditions on the faults. On the other hand, the three-dimensional velocity model that was newly constructed based on the results of surveys and observations for the comprehensive research (Yoshimi et al., JpGU-AGU2017). In this study, we use finite difference method (GMS, NIED) to calculate strong motion at the engineering bedrock considering the different fault parameters and hypocenters. This work is supported by the Comprehensive Research on the Beppu-Haneyama Fault Zone funded by the Ministry of Education, Culture, Sports, Science, and Technology (MEXT), Japan.

Keywords: Beppu-Haneyama Fault Zone, Dynamic Rupture, Strong Motion Simulation

Strong ground motions observed under the 2016 mid Tottori prefecture earthquake, Japan

*Takao Kagawa[1], Tatsuya Noguchi[1], Shohei Yoshida[1], Hiroshi Ueno[1], Sho Nakai[1], Kazu Yoshimi[1], shoya Arimura[1], Shinji Yamamoto[2]

1. Tottori University Graduate School of Engineering, 2. Tottori University Technical Division

October 21st., 2016, an earthquake with Mj 6.6 hit mid area of Tottori prefecture, Japan. Earthquake swarms have been activated in the area since mid October in 2015. Large number of seismometers installed by the prefectural government, JMA(Japan Meteorological Agency), NIED(National Institute for Earth Science and Disaster Resilience) and Tottori University, observed strong ground motions in the area. Aftershock observations were also conducted just after the main shock at several temporary sites in the area with housing damages. From prompt analysis of the observed strong motions, it is understood that the ground motions were affected strongly by local site conditions, especially their predominant period caused by sedimentary response. The observed predominant periods at strong motion sites agree well with those estimated by previously conducted microtremor observations in the target area. Characteristics of the observed ground motion and structural damages due to the earthquake are reported considering effect of surface geology in the area.

Keywords: The 2016 mid Tottori prefecture earthquake, Strong Ground Motion, Surface Geology

Damage Islands in Mashiki Town from the 2016 Kumamoto Earthquakes

*Masumi Yamada[1]

1. Disaster Prevention Research Institute, Kyoto University

The 2016 Kumamoto earthquakes caused serious building damage in the near-source regions. The first earthquake (foreshock, Mj6.5) occurred at 21:26, April 14 and the second event (mainshock, Mj7.3) occurred at 1:25, April 16. Since there was only a 28 hour interval between the two events, it is difficult to separate the damage of the two earthquakes from field surveys.

We analyzed aerial photos taken by the Geospatial Information Authority of Japan on the 15th and 16th of April and investigated the distribution of collapsed buildings along the Akitsu river. The photos cover the most severely damaged areas in Mashiki town. The two sets of photos taken between the foreshock and mainshock and after the mainshock, enable identification of the separate damage due to the foreshock and mainshock. The damage distribution is very heterogeneous, and the concentrations of severe damage occur in isolated areas resembling islands. The spatial pattern of the collapsed buildings due to the foreshock and mainshock were similar, but the number of collapsed buildings from the mainshock was 4 to 5 times the number for the foreshock.

The distribution of the collapsed buildings was compared with other information, such as the location of fault surface rupture, geomorphological map, and the location of the older built areas. The surface rupture was observed in the center of Mashiki town. The largest offset was about 40 cm along the southern edge of the concentrated damage area. Since this surface rupture was observed only after the mainshock, it is unlikely that the presence of the surface rupture generated the similar pattern of damage for the foreshock and mainshock in Mashiki.

Local geology in the survey area consists of the floodplain of the Akitsu river, multiple layers of river terraces, and an upper plateau of volcanic material. The heavily damaged area was in consistently in the lowest river terrace. The floodplain has the softest soil conditions in the area, but damage on the floodplain was much less than on the river terrace. The soft soil conditions are confirmed by microtremor array observations which showed thick sedimentary deposits with S-wave velocity less than 100 m/s on the floodplain. The observation that the most severe damage did not occur on the softest soil sites, is contradictory to many past studies. This unusual result needs further study to clarify the mechanisms of this damage distribution.

The damage islands correspond well to the distribution of the older built areas, which were constructed in the Meiji era (~1900s). Our photo analysis showed that the older buildings have a higher collapse ratio throughout the area. Therefore, building age and deterioration of the structures contribute to the damage distribution. The cause of the damage islands is likely due to a combination of the subsurface soil structure and age of buildings.

Keywords: kumamoto earthquake, building damage, strong motion

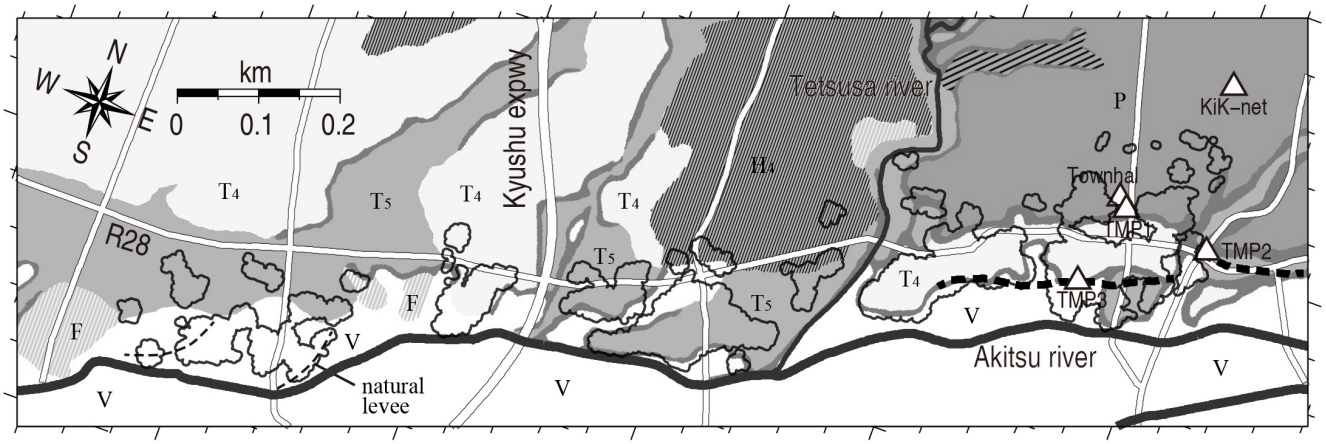

V: valley plain
F: fan and talus
T4: terrace surface 4
T5: terrace surface 5
H4: low relief hill composed of pyroclastic flow deposits
P: surface of pyroclastic flow plateau

A Study on anisotropy of shear wave velocity near the source region of the 2016 Kumamoto earthquake
-On the basis of seismic interferometry between ground surface and down hall of KiK-net observation-

*Kentaro Motoki[1], Kenichi Kato[1]

1. Kobori Research Complex

Some studies said that site amplification might affect destructive strong ground motions around Mashiki-Town according to results of aftershock observation and microtremor measurements. We evaluated subsurface structure models from microtremor array explorations, and explained that the resulted Vs structure models caused high amplitude of ground motions along NS direction, comparing between Mashiki-Town and just near a surface fault. The Vs models could not, however, reproduced strong motions along EW direction, and we found that different natural periods showed from each other horizontal direction at Mashiki Town (KMMH16). In this report, we investigated anisotropy of Vs near the source region of the 2016 Kumamoto earthquake, by applying seismic interferometry to KiK-net data.
We picked 3 stations, which are KMMH16, KMMH14 and KMMH03, as target sites. Resulted anisotropy parameters, which is $(v_{fast}-v_{slow})/v_{fast}$, are 0.22 at KMMH16, 0.23 at KMMH03 and 0.15 at KMMH14. This anisotropy might not be explained by irregularity of subsurface structure, because there were few changes in results of seismic interferometry by binned back azimuth.
We expect directional difference of stress field due to plate motion as a factor of anisotropy, because Nakata and Snieder(2012) showed that the fast shear wave direction correlated with the direction of the plate motion in Tohoku district, Japan. In near future, we will apply this investigation to a number of stations, and will construct subsurface structure model for each polarization direction considering with other explorations, e.g. receiver function and phase velocity.

Keywords: the 2016 Kumamoto earthquake, seismic interferometry, KiK-net, anisotropy of shear-wave velocity

Velocity Structure Model of Sedimentary Basins in Toyama Prefecture, Japan, by Microtremor Array Measurements

*Kimiyuki Asano[1], Kunikazu Yoshida[2], Ken Miyakoshi[2], Michihiro Ohori[3], Tomotaka Iwata[1]

1. Disaster Prevention Research Institute, Kyoto University, 2. Geo-Research Institute, 3. Research Institute of Nuclear Engineering, University of Fukui

Sedimentary plains or basins in Toyama prefecture such as the Toyama plain, the Imizu plain, and the Tonami plain consist of alluvium fans and coastal plains (Fujii, 1992). These sedimentary basins are filled by thick sedimentary layers with thickness of more than several km formed during and after the back-arc rifting of the Sea of Japan in Neogene time (Toyama prefecture, 1992). The bedrock belongs to the Hida metamorphic belt. Many active thrust faults exist along boundary between hills and plains. Sea floor active faults were also identified around the Toyama Trough (Ishiyama *et al.*, 2014). A reliable basin velocity structure model is indispensable for predicting strong ground motions from those onshore and offshore active faults. However, geophysical exploration to survey the S-wave velocity structure down to the seismic bedrock is very few in this area. Thus, we have conducted microtremor array measurements and estimated the S-wave velocity structure models in this area.

The microtremor array measurements were conducted at 15 sites on 27-31 October 2015, 10-13 November 2015, and 9-12 November 2016 (see a map attached). These sites are close to strong motion stations of K-NET, KiK-net, JMA and Toyama prefecture in Nyuzen town (NYZ), Uozu city (UOZ), Namerikawa city (NMK), Tateyama town (TTY), Toyama city (TYB, TYF, YTO, OYM), Imizu city (SIM, DIM, SNM), Tonami city (TNM), Nanto city (FKM, NNT), and Oyabe city (OYB). In order to obtain the S-wave velocity structure continuously from the ground surface to the seismic bedrock, a set of array measurements consisting of several different sizes of array from about 20 m to 1.5 km was conducted at each site. Each array consists of seven Lennartz LE-3D/5s seismometers. The vertial component of microtremor was analyzed by the spatial auto-correlation method (SPAC), and we obtained the phase velocity in the frequency range 0.2-5 Hz. Sites on alluvial fans, NYZ, UOZ, TTY, TYF, YTO, OYM, TNM, FKM, NNT, and OYB have relatively higher phase velocity (0.6-1.0 km/s) even at 2 Hz or higher. On the other hand, other sites (NMK, TYB, SIM, DIM, and SNM) have relatively lower phase velocities (0.2-0.5 km/s).

We estimated the S-wave velocity structure model for each site from the obtained phase velocities assuming that the observed phase velocity represents the fundamental mode of Rayleigh wave. We referred to the nation-wide three-dimensional velocity structure model J-SHIS V2 developed by NIED (Fujiwara *et al.*, 2012), and we assumed a layered velocity structure model composed of homogeneous sedimentary layers and bedrock. The S-wave velocity for each layer was fixed at the value given by J-SHIS V2 model, and we estimated thicknesses of these layers to fit the observed dispersion curve by the genetic algorithm (Yamanaka and Ishida, 1998). We included an additional surface layer above the layer of Vs 0.6 km/s for sites where low phase velocities were observed. We also added a layer of Vs 0.75 km/s for some stations considering data fits. The estimated velocity structure models explain the observed phase velocities better than the present J-SHIS V2 model. The depth of seismic bedrock is approximately 5-6 km in the Toyama and Tonami plains, which is consistent with the deep seismic reflection and refraction survey KT01 crossing the Tonami plain and the Kureha hill by Ishiyama *et al.* (2016).

We are planning to improve the three-dimensional velocity structure model in this area combining our results and other information such as reflection and refraction surveys.

Acknowledgements: This study was conducted by the integrated research project on seismic and tsunami hazards around the Sea of Japan funded by the Ministry of Education, Culture, Sports, Science and

Technology, Japan. The field observation was conducted with help by people participating from Geo-Analysis Institute, Geo-Research Institute and DPRI, Kyoto University.

Keywords: Toyama plain, velocity structure model, microtremor array measurement

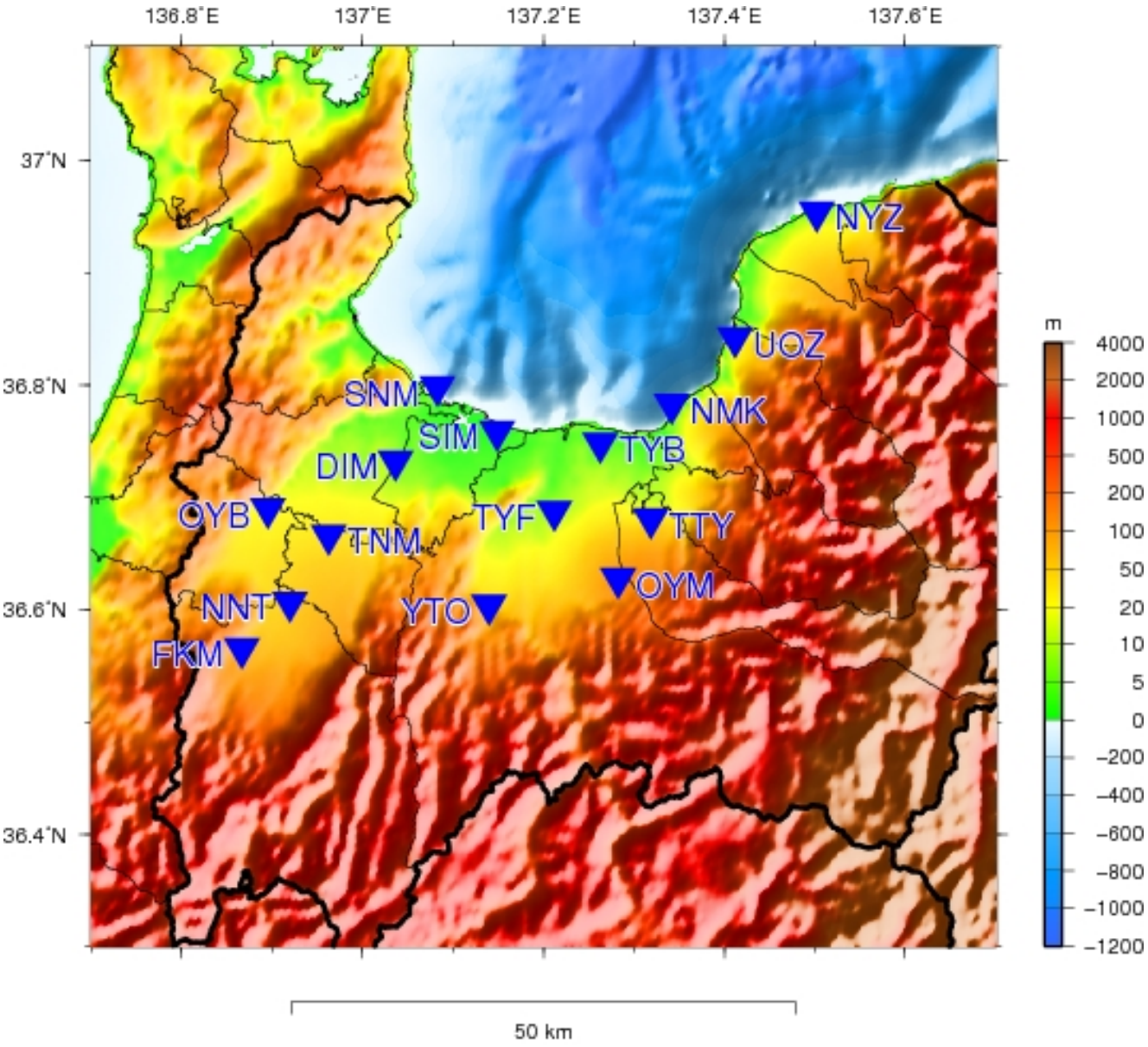

Modeling of the subsurface structure from the seismic bedrock to the ground surface for a broadband strong motion evaluation in Kanto Area. (part2)

*Shigeki Senna[1], Atsushi Wakai[1], Kaoru Jin[1], Hisanori Matsuyama[2], Takahiro Maeda[1], Hiroyuki Fujiwara[1]

1. National Research Institute for Earth Science and Disaster Resilience, 2. OYO Corp

We have collected a lot of boring exploration and physical property data (mainly microtremor observation ones) in the past, which are important to especially evaluate seismic ground motion in period range from 0.5 s to 2.0 s, and have studied combining a shallow part with a deep one on a subsurface structure model, for the purpose of modeling subsurface structure so that we can evaluate broadband earthquake ground motion from 0.1 Hz to 10 Hz. In this paper, we will report the methods of modeling initial subsurface structure and S-wave velocity structure which incorporate period and amplification characteristics based on earthquake and microtremor observation records, in the whole area of Kanto including Tokyo, Japan.

In this research, initial geological models were developed and then subsurface structure models from seismic bedrock to ground surface were constructed by using records of earthquake observation and microtremor array observation. These models in Kanto area were improved in terms of broadband period characteristics in comparison with the previous integrated models. In addition, about computation with 1D multiple reflection method executed separately, the results were considerably improved in the vicinity of period 1 s which was important from the standpoint of disaster prevention. It can result from not only detailed modeling of shallow subsurface structure by collecting soil columns data, but also improvement of models by evaluating phase velocity and H/V spectral ratio based on microtremor observation, for the structure around engineering bedrock from Vs300 m/s to Vs500 m/s which were boundary layers between shallow and deep subsurface structure.

There are a number of problems in terms of model quality variability by region due to collection density of boring data at the time of development of initial geological models. But the method, which has using miniature array observation etc. and modifying the depth of engineering bedrock surface with geological information, can enable an S-wave velocity model to be stably improved around engineering bedrock in any region. In the near future, we will develop subsurface structure models in Tokai area and all over Japan.

Keywords: Strong motion evaluation, S-wave velocity structure model, Microtremor array, Borehole data

Estimation of bedrock depth by receiver function using strong motion data in the Kyoto basin

Tomoya Shimomura[1], Kimiyuki Asano[1], *Tomotaka Iwata[1]

1. Disaster Prevention Research Institute, Kyoto University

We estimated R/V receiver functions of P waveforms of local earthquakes observed at strong motion stations in the Kyoto basin. Assuming a peak time of observed R/V receiver functions corresponds to the difference in arrival time between the direct P wave and the P-to-S converted wave (PS-P time) generated at the sediment/bedrock boundary in the Kyoto basin, we got the basin depth. The present Kyoto basin velocity model (Kyoto Prof., 2006) agreed with the obtained bedrock depth at most stations except several stations located near the basin edge. We modified the bedrock depth beneath each station. For validating that the peak time is corresponding to the PS-P time, we calculated theoretical R/V receiver functions using the discrete wavenumber method (Bouchon, 1981) with a double-couple point source in laterally homogeneous modified velocity model. Theoretical R/V receiver functions using the modified model showed good agreement to the observed R/V receiver functions.

Keywords: receiver function, Kyoto basin

Application of a fast calculation for full waves microtremor H/V based on diffuse field to identify underground velocity structures

*Hao Wu[1], Kazuaki Masaki[1], Kojiro Irikura[1], Francisco Jose Sanchez-Sesma[2]

1. Disaster Prevention Research Center, Aichi Institute of Technology, 2. Instituto de Ingenieria, Universidad Nacional Autonoma de Mexico

Based on Diffuse Field Approximation, the Full Waves (DFA-FW) Microtremor H/V Spectral Ratio (MHVSR) is expressed as the square root of imaginary part of the Green’ s functions in the horizontal component to that in the vertical component. The DFA-FW MHVSR evaluated with the underground velocity structures composed of PS logging data is found to be the best matching with the observed MHVSRs at some KiK-net stations, compared with the transfer function of SH waves, H/V spectral ratio of fundamental mode of Rayleigh waves (ellipticity), and H/V spectral ratio of surface waves including contributions from fundamental and higher modes of both Rayleigh and Love waves excited by distributed surface sources. Therefore, the DFA-FW MHVSR should be applied to identify the underground velocity structures at the interested sites.

However, the conventional methods, such as discrete wavenumber method and contour integration method, is very time consuming in calculating the imaginary part of the Green’ s functions. For a given layered medium, the DFA-FW MHVSR is found well approximated with only Surface Waves (DFA-SW) MHVSR of the “cap-layered medium” without fixed bottom which consists of the given layered medium and a large velocity cap layer in the deep added to the bottom of the given layered medium. Because the contribution of surface waves can be simply determined by residue theorem, the computation of DFA-SW MHVSR of cap-layered medium is significantly faster than that of DFA-FW MHVSR computed by other methods. The DFA-SW MHVSR of cap-layered medium, as a fast calculation for DFA-FW MHVSR of layered medium without cap layer, is then applied to identify the underground velocity structures above the bottom of the boreholes at KiK-net strong-motion stations.

The identified underground velocity structures between surface and bottom of boreholes were employed to evaluate DFA-FW MHVSRs which were consistent with the DFA-SW MHVSRs of corresponding cap-layered media. The earthquakes records at KiK-net stations provided the earthquake motions of H/V spectral ratios and spectral ratios of horizontal motions between surface and bottom of boreholes. The consistency between observed and theoretical spectral ratios for earthquake motions, indicated that the underground velocity structures identified from DFA-SW MHVSR of cap-layered medium were reasonable.

Keywords: microtremor H/V spectral ratio, diffuse field approximation, full waves, surface waves, cap layer, underground velocity structures

A study using waveform simulations on the applicability of seafloor strong motion records to the source process analysis

*Hisahiko Kubo[1], Shunsuke Takemura[1], Wataru Suzuki[1], Takashi Kunugi[1], Shin Aoi[1]

1. National Research Institute for Earth Science and Disaster Prevention

Because of the recent development of seafloor strong motion observation networks in the subduction zone of Japan such as DONET and S-net, seafloor strong motion records become available in the source process analysis. The use of seafloor records leads to the improvement in station coverage of the source process analysis for offshore earthquakes, which can improve the resolution and reliability of the analysis (e.g. Iida et al. 1988; Iida 1990). However, because of a limited knowledge on the offshore subsurface velocity structure, it is difficult to obtain Green's functions that can reproduce observed waveforms. Moreover, 1D synthetic waveforms, which are calculated with a 1D velocity structure model and widely used in conventional source-process analyses, are inappropriate to consider the offshore heterogeneous structure including a seawater, a rolling seafloor, thick sediments, and a subducting oceanic plate. One approach for this is to use 3D synthetic waveforms, which are calculated by 3D numerical simulations with a 3D velocity structure model; however the use of them is not easy because of a limited knowledge on the offshore structure and the high calculation cost. In this study, based on waveform simulations, we investigate the applicability of seafloor records to the source process analysis.

We prepare 3D synthetic waveforms for models with/without a seawater and 1D synthetic waveforms at S-net stations off Fukushima for near-coast and near-trench shallow crustal earthquakes in three period bands of 5-10 s, 10-25 s, and 25-50 s. 3D synthetic waveforms for a model with a seawater are calculated with a 3D FDM simulation (Takemura et al. 2015) assuming a 3D velocity structure model, which is based on the 3D subsurface structure model of J-SHIS (Fujiwara et al. 2009, 2012) including topographies and a seawater layer. 3D synthetic waveforms for a model without a seawater are calculated assuming a 3D velocity structure model, which is same as the above model but a seawater layer is replaced with an air. 1D synthetic waveforms are calculated at each station with the discrete wavenumber method (Bouchon 1981) and the reflection/transmission matrix method (Kennett and Kerry 1979) assuming a 1D velocity structure model for each station, which is extracted from the J-SHIS model.

To investigate the effect of a seawater layer, we compare the 3D synthetic waveforms for models with/without a seawater. Although the waveforms at transverse component are almost similar, the difference between their waveforms at radial and vertical components appears at periods lower than 25 s. The distribution of stations with the waveform difference depends on the horizontal event location: the waveform differences in the near-coast event are found at stations with a deep water depth, while these in the near-trench event are shown at almost all stations. Previous studies (e.g. Nakamura et al. 2014; Noguchi et al. 2016) demonstrated that the presence of a seawater and sediments leads to the excitation of oceanic Raleigh waves and that the predominant period of the fundamental mode of the Rayleigh waves depends on the seawater thickness. Our result and previous studies suggest that in the case of the near-trench earthquakes and/or the use of waveforms at stations with a deep seawater depth, appropriate waveform components and period band for the source process analysis are limited as long as Green's functions for a model without a seawater are used.

We also investigate how the 1D synthetic waveforms can reproduce the 3D synthetic waveforms considering the offshore heterogeneous structure. The waveform comparison suggests that although the amplitude difference and the time shift of S-wave and later phases are shown at many stations, there are stations that the phases of S-wave are similar. This suggests the possibility that seafloor records after the corrections of time shifts and amplitude differences can be used in the source process analysis.

Keywords: Seafloor strong motion records, Source process analysis, Waveform simulations

Source process of the October 21, 2016, Tottori-chubu earthquake

*Kazuhito Hikima[1]

1. Tokyo Electric Power Company Holdings, Inc.

<INTRODUCTION>
An M 6.6 earthquake occurred at 14:07 on October 21, 2016 in central Tottori Prefecture. During this earthquake, high acceleration records were observed within the source region. For example, JMA intensity 6- was recorded at TTR005 (K-NET, Kurayoshi), and the PGA at this station was about 1380 gal in EW component and 1490 gal in the synthetic of three components. The effect of surface geology is regarded as one of the reasons for these strong motions in general. However, two distinct wave packets are recognized in the observed waveforms in the near source region, and long period pulse like shape is dominant in the former packet, on the other hand, short period component is significant in latter packet. These observations suggest that the effects of the source process are not negligible for the strong motions. So a waveform inversion analysis was applied for this earthquake to consider the effect of the source process.

<OUTLINE of ANALYSIS>
We used the waveforms from 16 KiK-net borehole stations (by NIED) to reduce the effects of the surface geology. In Addition, two K-NET stations, TTR005 which is located immediately above the source region, and OKY015 which is located in the south of the source, were incorporated in the inversion analysis. The acceleration waveforms were filtered between 0.03 and 0.8 Hz, and were integrated to velocity waveforms for the inversion analyses.
The source processes were inverted by the multi time window analysis (Yoshida et al., 1996, Hikima, 2012). The Green’ s functions were calculated using 1-D velocity models, which were tuned by the waveform inversion method (Hikima and Koketsu, 2005), using the records of the Mw 4.1 event occurred on October 21. The fault planes of the initial models were configured by referring to the F-net mechanism solutions and the JMA hypocenter parameters. The final model was determined by considering the degree of fitness between the observed and synthetic waveforms. The size of subfaults for the inversion analyses were set in 2 km for preliminary trials, and in 1 km for the final result.

<RESULT>
The fault parameters were set tentatively as follows: the strike and the dip are 341 and 89 degree, and the length and the width are about 14 and 14 km, respectively. The depth of hypocenter is 10.6 km.
Left-lateral slip component is dominant, and the estimated moment magnitude (Mw) is about 6.2. A large slip area (asperity) was estimated around the hypocenter and its shallow part, in which the maximum slip was nearly 1.2 m. The rupture propagated toward the northern portion mainly, additionally a small asperity was estimated near the northern edge of the fault plane.

<DISCUSSION>
According to the inversion result, two asperities are obtained near the hypocenter and at the northern edge of the fault. So, it is considered plausible that these asperities are corresponding to the two wave packets observed in the waveforms. Furthermore, the larger asperity is existing between the hypocenter and the TTR005, so, the directivity effect from the asperity seems to be one of the reasons that caused the long period pulse waveform at the station. On the other hand, the short period component of the latter wave packet is the effect from the northern asperity, those slip velocity was comparatively large. Thus, it seems that the spatiotemporal source process obtained by the waveform inversion can explain the dominant characteristics of the observed waveforms.
We also calculated the stress change from the final slip distribution by using Okada's program. The stress

drop is at most 20 MPa, so, this value is comparable level with the past crustal earthquakes. This result indicates that the strong motion excitation of this earthquake was almost average level of other crustal earthquakes.

Keywords: Source process, Strong motion, Tottori-Chubu earthquake, Crustal earthquake

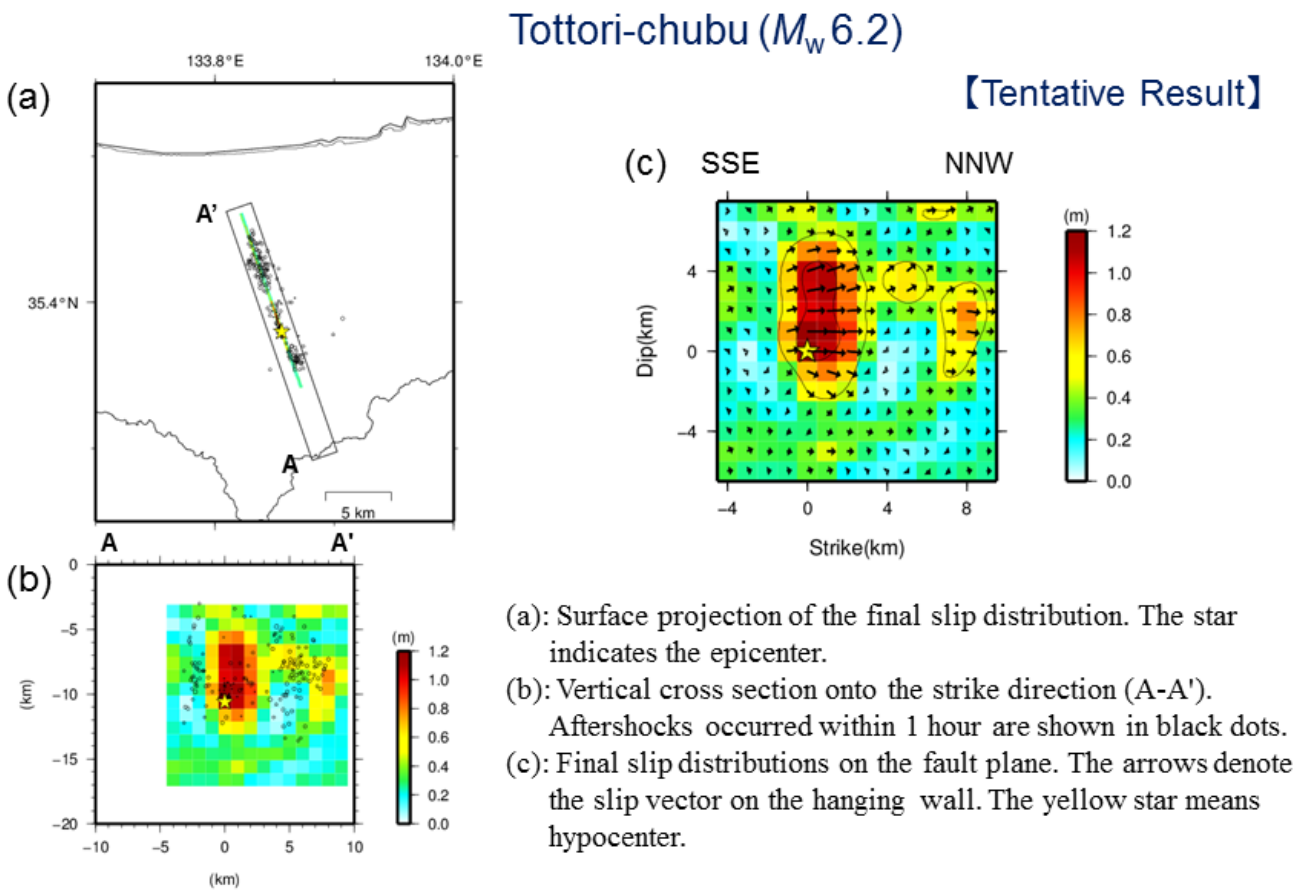

(a): Surface projection of the final slip distribution. The star indicates the epicenter.
(b): Vertical cross section onto the strike direction (A-A'). Aftershocks occurred within 1 hour are shown in black dots.
(c): Final slip distributions on the fault plane. The arrows denote the slip vector on the hanging wall. The yellow star means hypocenter.

Source model for the 2016 mid Tottori prefecture earthquake using Empirical Green's function

*Shohei Yoshida[1], Takao Kagawa[1], Tatsuya Noguchi[1]

1. Graduate School of Engineering, Tottori University

An earthquake of Mw6.2 occurred in the mid area of Tottori prefecture in Japan on October 21 2016. Several research institutions set large number seismometers, that obtained strong ground motions in the area. At several observation points recorded JMA seismic intensity of 6 lower, and partial area were suffered serious damages. Therefore we carry out aftershock and Micro-tremor observation to revel causes of the damages. We tried to estimate source model from those information. It is very important to reproduce the strong motion waveform at damage point for understanding reason of the damages and earthquake disaster mitigation in the future.In this study, we estimate source model of composed asperity through forward modeling with empirical green's function method. The target observation points were 8 in total that are maintained by NIED (K-NET, KiK-net) and Tottori prefecture. We selected foreshock event of Mw4.1 at 12:12 on October 21 2016 as an empirical green's function. The position of asperity was referred to previously conducted to heterogeneity slip distribution model, and each source parameters (e.g. rise time, rupture velocity) were determined by try and error. The estimated source model can reproduced the observed strong motion waveform. However, at several points are not sufficiently reproduced. In order to improve reproducibility of observed strong motion, it needs more detailed examination.

Keywords: 2016 mid Tottori prefecture earthquake, Source model, Empirical green's function

Source inversion using empirical Green's functions for the 2016 Tottori earthquake (Mj 6.6)

*Yoshiaki Shiba[1]

1. Central Research Institute of Electric Power Industry

During the 2016 Tottori earthquake on October 21, the peak ground accelerations at K-NET Kurayoshi (TTR005) reached 1381 gal. Since the station is located just above faulting area, spatial and temporal source rupture process would strongly affect the strong motions at TTR005. The response spectrum calculated from the strong motion record of TTR005 shows relatively large amplitude in the frequency range higher than 1 Hz, therefore the analysis of source process should take into account such higher frequency ground motions. In this study the inversion method using empirical Green's functions is adopted for the source modeling of the Tottori earthquake in order to evaluate broadband ground motions.

From the aftershock distribution and CMT solution of the main shock estimated by F-net, we assumed the left-lateral fault plane model with the strike in the NS direction and the nearly vertical dip angle. Observed records from the aftershocks of Mj 4.0 occurring just beneath TTR005 were used for the empirical Green's functions. Velocity motions of two horizontal components for KiK-net subsurface stations and near-source K-NET stations are used for the source inversion in the frequency range from 0.2 to 2 Hz. Once the moment density distribution on the fault plane is estimated, the effective stress is searched with moment density simultaneously by using the histogram of estimated model parameters as prior probability distribution for the inversion procedure.

The obtained source model indicates large slips mainly in the shallow area around the hypocenter and secondary large slips just beneath TTR005 station, which is located about 5 km north of the epicenter. Estimated rise time on the fault plane is as short as 1.6 seconds at maximum. From the slip distribution of the main shock, it suggests that strong motions at TTR005 area radiated from these two SMGAs sequentially. In case of inversion analysis without records of TTR005, the secondary large slip does not vanish in the estimated source model.

The simultaneous inversion of effective stress and moment density revealed that the shallow large slip area beneath TTR005 shows relatively small effective stress, while the asperity near the hypocenter implies also large effective stress. It is considered to be consistent with the empirical relation that shallow SMGA tends to show small stress drop compared to deep SMGA.

Keywords: 2016 Tottori earthquake, source model, empirical Green's function, strong ground motion

Source imaging of the 2016 Kumamoto earthquake by back-projection of near-filed P wave records.

*Mitsutaka Oshima[1]

1. Shimizu corporation

A series of strong ground motion caused by 2016 Kumamoto earthquake (hereafter, Kumamoto earthquake) devastated the areas along Futagawa-Hinagu fault zone and strong ground shake with Japan Meteorological Agency Seismic Intensity Scale 7 was observed twice for the first time in domestic history of earthquake observation.
Several studies on the spatio-temporal slip distributions have been reported based on waveform inversion pointing out heterogeneity of rupture process, such as depth dependency of slip velocity function.
The direction and the speed at which fault rupture proceeds, as is well known, controls major feature of ground motion around the causal faults. About the Kumamoto earthquake, spatio-temporal distribution of seismic wave emission has been studied by several researchers and those results show that the rupture propagated across fault planes with different strike and dip. Abrupt acceleration of rupture speed has also reported and these fact features the heterogeneity of fault rupturing occurred during the Kumamoto earthquake.
Although rupture heterogeneity strongly affects strong ground motion, it has been only partially taken into account in the current framework of strong ground motion prediction. Slip velocity function and rupture velocity variable on the fault planes are expected to be take into consideration in the future strong ground motion evaluation, and actually, some attempts to incorporate such heterogeneity in fault models for ground motion prediction are under way in the world. Hence, accumulation of information on fault rupturing process is essential to constitute a heterogeneous source model. In this study, I applied back-projection technique to reveal the time history of seismic wave emission during the Kumamoto earthquake.
Strong motion records recorded at 27 KiK-net and K-NET stations within 100km hyopocentral distance were used. Waveforms were rotated according to seismometer orientation and offsets were removed. Then the records were integrated into velocity by lattice filter of Kinoshita(1986). Traveltime data were processed in the similar way as Takenaka and Yamamoto(2004) to obtain seismic emission image with more precision in relative location. Further correction for travel time data was made by using the difference between observed and calculated traveltime from the hypocenter.
The back-projection technique used in this study is similar to that by Kao and Shan(2004), and Ishii et al.(2005). Waveforms were stacked with a combination of Hann window and N-th root stacking. The fault plane was determined from distribution of aftershocks although no assumption for fault plane is necessary in back-projection method.
As a result, some image of rupture propagation from Takano-Shirahata segment of the Hinagu fault zone to Futagawa segment of the Futagawa fault zone was obtained, where the strike and the dip of those two fault planes are different. The rupture rapidly increased its seismic wave emission while it’s moving toward northeast. However, both accuracy and resolution of the present results still leave plenty of scope for improvement. In the future study, I am planning to scrutinize data and data processing techniques, such as traveltime data and waveform stacking methods to get more exact and high-resolution image of the source process.

Acknowledgement: I would like to express my gratitude to NIED for providing me with KiK-net and K-NET data.

Keywords: back-projection , source imaging, Kumamoto earthquake

Study on spectral decay characteristics in high frequency range of observed records during The 2016 Kumamoto Earthquakes

*Masato Tsurugi[1], Takao Kagawa[2], Kojiro Irikura[3]

1. Geo-Research Institute, 2. Tottori University, 3. Aichi Institute of Technology

Spectral decay characteristics of ground motions for the 2016 Kumamoto earthquakes are examined. In this study, spectral decay characteristics in high frequency range are evaluated by two approaches. One is f_{max} filter, the other is spectral decay parameter, κ (Kappa).
In result, f_{max}'s of large earthquakes are estimated to be 7Hz to 10Hz and the larger earthquakes are, the smaller f_{max}'s tend to be. The power coefficient of f_{max} filter, s, of largest foreshock and mainshock of the 2016 Kumamoto Earthquake are larger than those of large earthquakes occurred in other region. From this result, a region dependency of spectral decay characteristic is suggested.
κ's of large earthquakes are estimated to be 0.0466 to 0.0482. There are positive correlation between s as power coefficient of high-frequency decay of f_{max} filter and κ as spectral decay parameter and between f_{max} for the f_{max} filter and f_E for parameter κ. f_E is a frequency at which spectrum starts to decrease on log-linear scale. f_E is a very important parameter for strong ground motion prediction, however f_E has not been examined carefully enough in previous κ studies. It is confirmed that evaluated high frequency characteristics by f_{max} filter and those from spectral decay parameter, κ agree well with each other.

Keywords: The 2016 Kumamoto Earthquakes, Spectral decay characteristics, fmax filter, Kappa

Appropriate Q value model in the Kanto region for simulating long-period ground motion

*Takahiro Maeda[1], Nobuyuki Morikawa[1], Asako Iwaki[1], Hiroyuki Fujiwara[1]

1. National Research Institute for Earth Science and Disaster Resilience

In this study, we investigate an appropriate Q-value model in the Kanto region for evaluating the ground motion on the engineering bedrock that has S-wave velocity of about 350 m/s by comparing the simulated ground motion with the observed data.

We use the ground-motion simulator (GMS; Aoi et al., 2004) which is a practical tool for seismic wave propagation simulation based on 3D finite difference method with fourth order of accuracy in space and second order in time using discontinuous grids. In the GMS, a method to introduce an anelastic attenuation effect easily in the time domain proposed by Graves (1996) is adopted. In this method, an attenuation function for S wave, $a(x,y,z)=\exp(-\pi f_0 \Delta t/Q_S(x,y,z))$, where Q_S is the spatially variable Q value for S wave, f_0 is the reference frequency and Δt is a time interval, is multiplied to the velocity and stress fields at each time step to introduce the anelastic attenuation. Since the Graves' s method is widely used, we examine the suitable Q value for applying the Graves' s method.

The velocity structure model used in this study is a shallow-deep integrated velocity structure model constructed in the Kanto region by integrating shallow structure (Vs < 350m/s) and deep structure. This velocity structure model was verified by comparing the observed and simulated ground motions of M4-5 earthquakes (Maeda et al., 2015, SSJ). In this verification, emphasis is placed on the reproduction of the periodic characteristics of the ground motion caused by the subsurface structure, and thus a goodness of fit between the observed and simulated ground motion is evaluated in the periodic domain using the Fourier spectral ratio. In the evaluation of the degree of fit, referring to the criteria of the SCEC broadband platform validation exercise (Goulet et al., 2015; Dreger et al., 2015), it is judged that the goodness of fit is high when the spectral ratio is within the range of 1/1.4 to 1.4, while the fit is low when the ratio is 1/2 or less, or 2 or more. Averages of spectral ratios calculated from all the data of 5 earthquakes recorded at 197 observation points and averaged spectral ratio at each observation point are within the range of 1/1.4 to 1.4 in the period range of 2 to 10 second. The verification shows that the shallow-deep integrated velocity structure model has been confirmed to be a highly descriptive model of the observed data. However, the period dependence that the amplitude of the simulated spectra is larger than that of the observed one at the shorter period range is recognized, suggesting the possibility of improving the goodness of fit by changing Q value. Therefore, we set up several Q value models to investigate whether the goodness of fit is improved.

In past studies, the Q value model in which $Q_0(=Q_S)$ is proportional to S-wave velocity as $Q_0=\alpha V_S$ (the unit of V_S is m/s) is adopted. For example, $\alpha=0.2$ is assumed in the Japan Integrated Velocity Structure Model (Koketsu et al., 2008; Earthquake Research Committee, 2012). In this study, we use the Q value model proportional to the S-wave velocity and assume that $\alpha=0.1$, 0.2, 0.5, 1.0, and the reference period ($T_0=1/f_0$) is 3 s. Among them, the setting of $\alpha=0.2$ is the same setting as the above verification. Qualitatively, as α decreases, the effect of attenuation due to Q value increases, so the amplitude of the simulated spectra decreases. As a result of investigating the change of averaged spectral ratio of all the data, the change in α is affecting spectral ratio particularly at the shorter period range and thus it is confirmed that the goodness of fit is improve by setting $\alpha=0.1$. In addition, the average value of the

spectral ratio for each observation point also tended to be close to 1 when $\alpha = 0.1$.
Furthermore, in addition to the study in the frequency domain above, we also study in the time domain focusing on the duration. Comparing the envelope shapes of the velocity waveforms of observed and simulated records, it is possible to roughly explain the decay characteristics of observed data using the Q value model set in this study. However, since the data length of the observed data is not enough, consideration of an appropriate α in the time domain is a future task.

Acknowledgement This study was supported by “Support Program for Long-Period Ground Motion Hazard Maps” of the Ministry of Education, Culture, Sports, Science and Technology (MEXT).

Keywords: Q model, shallow-deep integrated velocity structure model, long-period ground motion, GMS

Studies on Qs at the northern part of Kyushu district in Japan.

*kenichi Nakano[1], Shigeki Sakai[1]

1. HAZAMA ANDO CORPORATION

We have reported the variability of Qs in southern part of the Kyushu district, in the previous paper. In that paper, we used seismograms, which are from the M4-5 small-adequate scale earthquake observed by K-NET and KiK-net operated by the National Research Institute for Earth Science and Disaster Resilience, for evaluating the Qs in those areas. As a result, it showed that the average apparent Qs of the line, connecting the seismic source location to the earthquake catalog of JMA and the observation point, changes significantly, depending on regions (route combination of propagations). This suggests that it is necessary to use an appropriate Qs model in the target area, for strong ground motion simulations based on the statistical Green's function method or the like, for example.

In this paper, we evaluate the Qs for the northern part of Kyushu, as the damping properties, using the twofold spectral ratio method. First, the northern part of the Kyushu district was divided into “Region A” and “Region B” as shown by the light orange hatch in Fig. 1. In addition, the area in the southwestern part of the Kyushu district was indicated as “Region C” with a light blue hatch (we had already reported the Qs to the area in our previous paper). In the figure, epicenter distributions of the events occurred after the 2016 Kumamoto earthquake (April 14, 2016 to April 30, 2016) are showed as hollow circles, and red triangles also indicate seismic observation points in NET & KiK-net. The location of the epicenter is referenced to the JMA earthquake catalog. In the area shown in the figure, the evaluation of Qs was carried out in an area having a planar spread (Area), and as a propagation route (Line) respectively. However, since it was difficult to set the Area for “Region B”, only evaluation in Line was carried out. The name of each analysis case was written like “Region A-Area” or “Region A-Line”.

The results are shown in Fig. 2. As can be seen from this figure, it is clear that different Qs models are evaluated in Area-case and Line-case at each region, and also, Qs models are very similar in “Region A” and “Region C”. On the other hand, “Region B” is very different from other regions, Qs = 20*f^1.0 is evaluated. This model agrees to the Qs estimated by Izutani (2000), he assumes the propagation path as just under Mt. Krishima. The propagation path of “Region B” in this study is just under Mt. Aso because we want to secure the propagation distance. Lin et al. (2016) reports the existence of magma chamber from 5km to 10km depth under Mt. Aso. These facts suggest us the possibility that Qs model of “Region B” follows the same theory they pointed out. The Qs models in other regions are harmonious with the one estimated by Uchiyama and Yamamoto (2016). However, it is different from the value evaluated by Nakano et al. (2015). It seems to be due to the fact that the conditions, for example hypocentral distance, are different, and the area to be analyzed is also greatly different. In fact, we also conducted generalized spectral inversion analysis, under conditions tailored to Uchiyama and Yamamoto (2016) and Sato (2016), and confirmed that the Qs model estimated by the analysis is the same as the one proposed by Uchiyama and Yamamoto (2016).

Since our results include only small number of earthquakes and the area to be analyzed, we have to continue the investigation for studying attenuation properties to perform the analysis, considering the variability of earthquakes and propagation path. As our future tasks, we plan to develop a method for evaluating complex damping structures in order to improve the accuracy of strong ground motion prediction.

Acknowledgements: We used the strong motion records provided by National Research Institute for Earth Science and Disaster Resilience (NIED) in this study. We gratefully appreciated it.

Keywords: Qs, Propagation pass, Twofold spectral ratio method

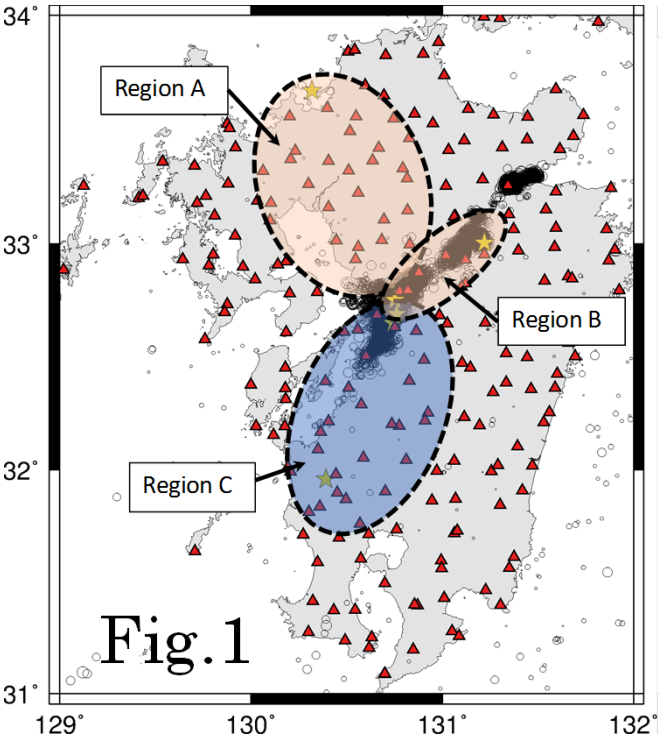

Fig.1

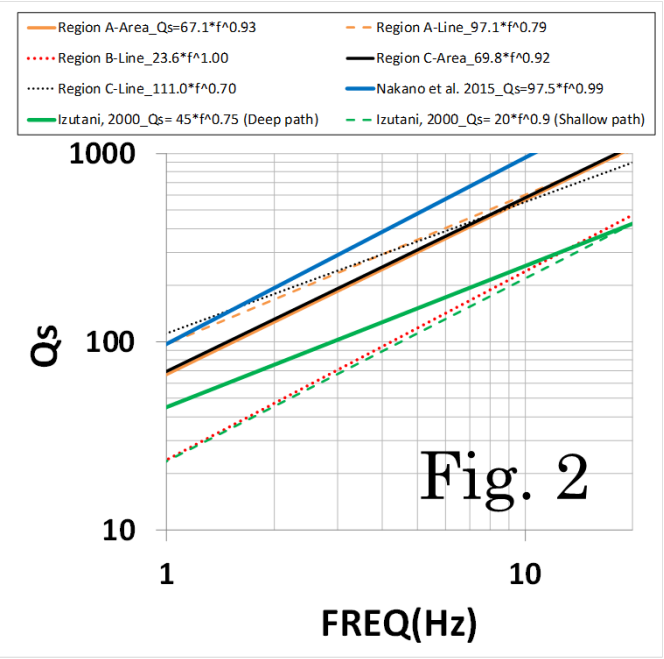

Fig. 2

A New Multidimensional Attenuation Relationship for Instrumental Seismic Intensity

*Hiroto Tanaka[1], Ritsuko S. Matsu'ura[2], Mitsuko Furumura[2], Tsutomu Takahama[1]

1. Kozo Keikaku Engineering Inc., 2. Earthquake Research Center, Association for the Development of Earthquake Prediction

Matsu’ura et al. (2011) and Noda et al. (2016) proposed a multidimensional attenuation relationship of the velocity response spectra for wide range of distance and period, by using the attenuation term proportional to depth of subducting slab. In this study we propose an attenuation relationship for JMA seismic intensity in the same way.
We constructed database using strong-motion records from K-NET and KiK-net, which have peak ground velocity of 0.1 cm/s or more. The database was divided into three groups by seismic source types of Inter-Plate, Intra-Plate, and Very Shallow (VS) earthquakes in Japan. Inter- and Intra-Plate earthquakes occurred on and in subducting Pacific plate. We used the same formula of attenuation relationship as that of velocity response spectra after comparing trends of seismic attenuation between the velocity response and instrumental seismic intensity.

$$INT = Ac + Aw \cdot Mw - b \cdot \Delta - \beta \cdot \log(\Delta) - d \cdot \min(\delta, 250) \pm \sigma$$

where INT is instrumental seismic intensity, Mw is moment magnitude, Δ is hypocentral distance (km), and δ is depth of upper boundary of the Pacific plate. Ac, Aw, b, β and d are regression coefficients, and σ is standard deviation. For earthquakes with Mw > 7.5, we adopted Δ that is closest distance to the fault rupture. We set the upper limit of δ at around 250 km depth, and it improved the consistency with observation. The coefficient β in the attenuation term which is proportional to $\log(\Delta)$ is often fixed around 2 in other previous studies of attenuation relationship for INT, but in this study we estimated β by regression analysis. The final combination of regression coefficients was determined by AIC, because the optimal combination depends on the seismic source type.
For Inter-Plate, the combination of coefficients Ac, Aw, b, β and d got an optimal solution. The standard deviation in the case using the combination was 0.643 and the AIC was also superior, whereas that using conventional simple form (combination of Ac, Aw, b, β) was 0.691. For Intra-Plate, the combination of coefficients Ac, Aw, β and d got an optimal solution. The attenuation relationship of Intra-Plate could explain the observation by the attenuation terms of coefficient β and d (without coefficient b) because there was few data at the short distance. The standard deviation in the case using the combination of Ac, Aw, β and d was 0.644, whereas that using combination of Ac, Aw, b and β was 0.751. For the Inter- and Intra-Plate, we found that the attenuation term proportional to δ was an effective term to account for the difference in attenuation such as anomalous seismic intensity distribution. On the other hand, for VS, the term proportional to δ was not effective, and the combination of coefficients Ac, Aw, b, β was got an optimal solution with standard deviation of 0.677.
We compared these results with observed one or other previous studies in order to verify the obtained relationship. In the Inter- and Intra-Plate earthquakes using the attenuation term proportional to the plate depth in this study, the residuals between observed and predicted by this study is smaller than that by other studies over a wide range of distances. On the other hand, in VS earthquakes without attenuation term proportional to plate depth in this study, the seismic intensity predicted by this study and by other studies are in the same range, and the difference of the residuals between the predicted and observed of for each study was small. These suggest that the attenuation term proportional to δ in this study is

effective to explain observed data.
We will perform further study for a correction term of ground amplification to predict seismic intensity more accurately at arbitrary sites.This study was conducted as an entrusted research from Ministry of Education, Culture, Sports, Science and Technology. We used strong-motion records from NIED K-NET and KiK-net.

Keywords: Ground Motion Prediction Equation (GMPE), Attenuation term proportional to plate depth, Selection by AIC

Type	*Ac*	*Aw*	*b*	β	*d*	σ
VS	2.096	0.962	0.00287	2.409	-	0.677
Inter-Plate	4.726	0.674	0.00171	2.416	0.00527	0.643
Intra-Plate	2.509	1.444	-	3.576	0.00883	0.644

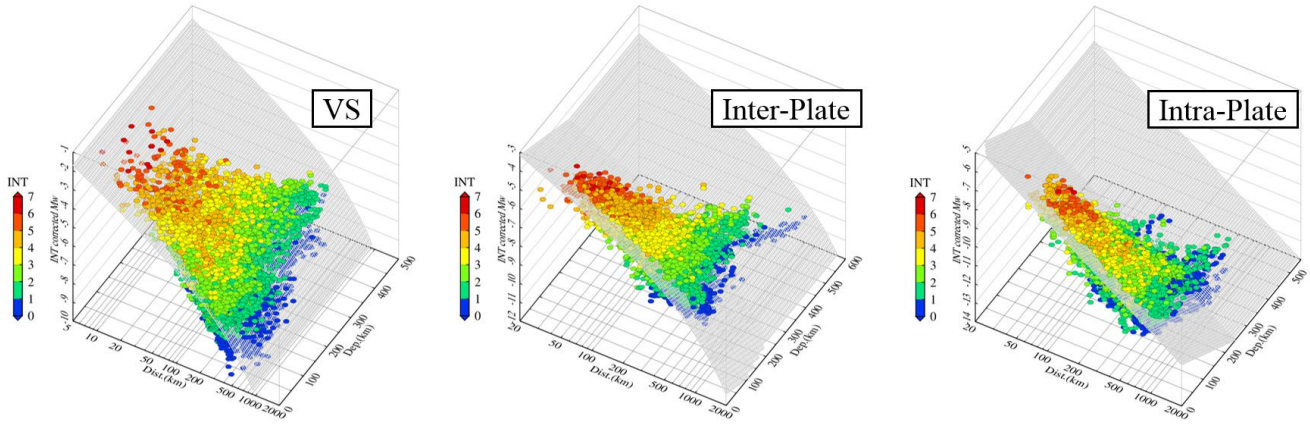

Seismic activity modeling of earthquakes occurred on inland active faults with smaller magnitude than assumed characteristic event for probabilistic seismic hazard

*Jun'ichi Miyakoshi[1], Takeshi Morii[2], Mitsutaka Oshima[2], Nobuyuki Morikawa[3], Hiroyuki Fujiwara[3]

1. Ohsaki Research Institute, Inc., 2. Shimizu Corporation, 3. National Research Institute for Earth Science and Disaster Resilience

In this study, we model seismic activity of earthquakes occurred on inland active faults with smaller magnitude than assumed characteristic event for probabilistic seismic hazard. Examples of these earthquakes are northern Nagano prefecture earthquake in 2014 (M6.7) and Kumamoto earthquake in 2016 (M6.4).
For a part of these earthquakes, probabilistic seismic hazard map by the Headquarters for Earthquake Research Promotion (HERP) are modeled seismic activity of earthquakes that does not show signs on the surface. We consider three new models for these earthquakes referred to the model of HERP. In the model of HERP, the upper limit of magnitude is assumed characteristic event on active fault or 7.4, the lower limit of magnitude is 6.8, and the mean recurrence interval is twice the interval of the active fault. In Model 1, the lower limit of magnitude is 6.5 among the model of HERP. In Model 2, the mean recurrence interval is equal to the interval of the active fault among the model of HERP. Model 3 is combined Model 1 and Model 2.
We calculate probabilistic seismic hazard map based on three new models. As a result, the seismic hazard of Model 3 is the largest, and the seismic hazards of Model 1 and Model 2 are comparable.

Seismic intensity distribution and validation of the source location and the magnitude of the 1914 Sakurajima earthquake

*Reiji Kobayashi[1], Yukina Furuya[2,3], Hiroki Kuwahara[2]

1. Graduate School of Science and Engineering, Kagoshima University, 2. Faculty of Science, Kagoshima University, 3. Grand Lacere Kagoshima

The 1914 Sakurajima earthquake (M 7.1) occurred about eight hours after the eruption of Sakurajima. The seismic intensity distribution in Kagoshima city is estimated from the damaged data of houses and stone block walls (Imamura, 1920). The intensity data used in Imamura (1920) is originally defined in his study and cannot be directly compared to the present seismic intensity scale in Japan defined by the Japan Meteorological Agency (JMA) in 1996. Takemura and Toraya (2015) proposed a conversion procedure from damage data of houses to the present seismic intensity scale for the 1944 Tonankai earthquake.

The seismic intensity distribution in Kyushu Island has also compiled by Imamura (1920) and its isoseismal maps were drawn by Imamura (1920) and Omori (1922). The intensity data can be compared to the present seismic intensity in JMA scale, because the present seismic intensity scale was revised several times from that used for the isoseimal map for the Kyushu Island in Imamura (1920).

In this study, we convert from the damage data of houses in Kagoshima city (Imamura, 1920) to the present seismic intensity in the JMA scale. We also review the seismic intensity distribution in Kyushu Island. Then we verify the source location and magnitude using an attenuation relation of seismic intensity for Japan presented by Morikawa et al. (2010).

Imamura (1920) presents the total number of households but does not present the total number of houses. The sum of the completely destroyed, half destroyed, and partially damaged houses are larger than the number of household in a town, Shiomi-cho. We adopt two assumptions for the total number of houses. One is that the total number of houses in each town is equal to that of householders in it. The other is that the ratio of total number of houses to that of householders in each town is equal to the ratio in Shiomi-cho. The true value may be between those inferred from the two assumptions. The distribution of the present seismic intensity scale adopting the former assumption shows that the maximum intensity is 6 Upper, and that adopting the later assumption is that the maximum intensity is 6 Lower. The maximum difference between the intensities at a same place adopting the two assumptions is one grade.

We also plot the seismic intensities in Kyushu Island to review the isoseismal maps of Imamura (1920) and Omori (1922). The isoseismal contours of both papers are inconsistent to the intensity data at several observation points. It is difficult to draw the isoseismal contours being consistent with the seismic intensity data.

We verify the source location and magnitude of the 1914 earthquake. The source fault of the 1914 Sakurajima earthquake has not been investigated in previous studies. Kagoshima Prefecture assumes a source fault for the same type of an earthquake as the 1914 Sakurajima earthquake to predict the strong ground motions for disaster prevention. The seismic intensities predicted by the attenuation relation with Mw 7.1 are much higher than the observed ones in Kagoshima city. When the magnitude is fixed at Mw

7.1, the source fault location should be moved at least 50 km further from the assumed fault. If the source fault location is fixed, the magnitude should be 5.6. The comparison of the predicted seismic intensity to the observed ones in Kyushu Island shows that Mw 7.1 is too large.

Keywords: The 1914 Sakurajima earthquake, seismic intensity, magnitude

Seismic Intensity Distribution of the 1889 Meiji Kumamoto Earthquake

Noriko Niida[2], *Yoshiko Yamanaka[1]

1. Graduate School of Encironmental Studies, University of NAGOYA, 2. Department of Earth & Planetary Sciences, University of NAGOYA

We investigated historical earthquakes in the Kumamoto Prefecture. We collected historical earthquake information in the history books of the prefecture or the municipalities, historical newspapers, and Official Gazette.
On July 28th 1889 (Meiji 22), the earthquake (M=6.3) occurred at the west of Kumamoto city. Damage statistics on each municipality are reported in Official Gazette. Using seismic damage of house, bridge and crack in the ground, we estimated seismic intensity based on the relationship between seismic intensity and seismic damages proposed by Usami(2016) and obtained the distribution of seismic intensity of this event. The obtained seismic intensity map was compared with the site amplification factor data by National Research Institute for Earth Science and Disaster Resilience (NIED). It seems that the region which have larger site amplification factor tends to become higher seismic intensity.
Takemura(2016) estimated seismic intensity distribution from the collapsed houses reported by Imamura(1920) . His seismic intensity distribution almost resembles one in this study. In some area, seismic intensity of this study came to have a bigger 2-3 rank as his result. Because we estimated seismic intensity from damage of bridges and crack in the ground as well as the damage of the house, our estimated seismic intensities become a little bigger. Houses in the Meiji period were generally located on relatively strong ground which have small value of amplification factor. On the other hand, bridges often stand on the weak ground.
We concluded that seismic intensity determined from damage of houses sometimes becomes smaller than that from damage of other structures.

Keywords: the 1889 Meiji Kumamoto Earthquake, Seismic Intensity Distribution

Simulation of Long-Period Ground Motion in Damaged Areas during the 2016 Kumamoto Earthquake

*Kengo Muroi[1], Hiroaki Yamanaka[1], Kosuke Chimoto[1], Seiji Tsuno[2], Hiroe Miyake[3], Nobuyuki Yamada[4]

1. Tokyo Institute of Technology Department of Environmental Science and Technology, 2. Railway Technical Research Institute, 3. Earthquake Research Institute, University of Tokyo, 4. University of Teacher Education Fukuoka

The 2016 Kumamoto earthquake contains a foreshock with a Mj of 6.5 on April 14 and the main shock with a Mj of 7.3 on April 16. The earthquakes generated ground motions with a seismic intensity of 7 on the Japan Meteorological Agency twice in Mashiki,Kumamoto,Japan and many wooden houses were collapsed. In this study we conducted a simulation of strong ground motion during aftershocks of the 2016 Kumamoto earthquake, using subsurface structural model by Headquarters for Earthquake Research Promotion and GMS, and evaluated earthquake ground motion in the damaged areas. We assumed homogeneous fault model from a group of point sources. We used the aftershock with a Mj of 5.5 and a depth of 10km on April 19. First, we compare the waveform of rock site (KMM014). The calculated waveform has similar characteristics of the observed waveforms. Then, we compare observed ground motion records by Yamanaka et al. (2016) in the damaged areas with the calculated waveforms. The calculated waveforms in the damaged areas have similar characteristics of the observed waveforms which are characterized by long-period S-wave after initial S-wave in about 5 seconds. We also found high correlation between the amplitude of the ground motion and the damages at some observation points.

Keywords: Kumamoto Earthquake, Simulation of ground motion, Strong ground motion

A Study on Characteristics of Long-Period Ground Motion in the Kathmandu Valley during the 2015 Gorkha Nepal earthquake aftershocks

*Michiko Shigefuji[1], Nobuo Takai[2], Subeg Bijukchhen[2], Masayoshi Ichiyanagi[2], Tsutomu Sasatani[2]

1. Kyushu University, 2. Hokkaido University

The Indian Plate underthrusts the Eurasian Plate resulting in occurrence of a number of large earthquakes in the Nepal Himalaya. The Kathmandu Valley is formed by drying of a paleo-lake and consists of thick soft sediment below the center of city. We have installed a strong motion east-west line array observation (four sites; one rock site and three sedimentary sites) in the valley, on 2011, to understand the site effects of the valley. On 25 April 2015, a large M_W 7.8 earthquake occurred along the Himalayan front. The epicenter was near the Gorkha region, 80 km north-west of the Kathmandu Valley, and the rupture propagated eastward from the epicentral region passing through the valley and reached about 80 km north-east of the valley. The aftershock of M_W 6.6 occurred on 25 April 2015 ~80 km northwest of Kathmandu at epicenter near to that of the main shock. The other three large aftershocks were originated ~80 km east of Kathmandu; the aftershock of M_W 6.7 occurred on 26 April 2015 and the aftershocks of M_W 7.3 and M_W 6.3 occurred on 12 May 2015. The ensuing aftershock activities are concentrated in the eastern part of the rupture area. After the mainshock, we installed additional four stations on sedimentary sites on 05 May 2015. We discuss the characteristics of long-period ground motion in the Kathmandu Valley based on these strong motion records from large aftershocks ($M_W > 6$).

The acceleration waveforms at the sedimentary sites are longer and larger than those at the rock site. We checked acceleration Fourier spectra of 40.96 sec of S-wave with rotated acceleration records for each sites and compared between the rock site and other sedimentary sites. In high frequency range (around 0.2 Hz ~), we can observe the strong amplification factor in each site condition. On the other hand, the amplification are extremely small in low frequency (~ around 0.2 Hz) on horizontal components, whereas amplitude are almost same on vertical component. In low frequency range, the spectra have peak in 0.1 ~ 0.2 Hz even in the rock site. Furthermore, the spectral shape on the low frequency range is proportional not to the square but to the cube of frequency. The transition frequency is around 0.2 Hz, but this frequency has small variations by earthquake. Regarding M_W 7.3, M_W 6.3 aftershocks, vertical components semblance analysis show that 0.1 Hz waves are propagated from epicenter with 3 km/sec phase velocity. The particle motion of vertical-radial component shows the retrograde motion which is fundamental Rayleigh wave.

Considering the shape of spectra in low frequency range, we tried to calculate 1-D theoretical waveforms by the discrete wave number method (Takeo, 1985) with 1-D velocity structure (Crust1.0; Laske *et al.*, 2013) and GCMT source mechanism. By this simulation, the surface waves are contained in the analyzed time window; Rayleigh and Love waves which have 0.1 Hz power reached just after direct S-wave initial motion. Therefore, we understood that the shape of the low frequency range are affected by these surface waves.

Spectral ratios of the sedimentary sites to rock site have different dominant frequency (0.2 ~ 0.8 Hz) and amplitude at each sites. These differences of the spectral shape in closed area speculate the complexity

of the basin structure. The predominant frequencies of the spectra could be roughly explained by theoretical response based on 1-D structures made with geological data and gravity anomaly data (Bijukchhen *et al.*, 2016).

During examination of long period motion on large aftershocks, the characteristics are strongly affected by surface wave. We will study the excitation and propagation of surface wave of the Kathmandu basin extensively, try to examine the amplification characteristics quantitatively, and construct the velocity structure of each site in detail.

Keywords: The 2015 Gorkha Nepal earthquake aftershocks, Kathmandu Valley, Long-Period Ground Motion

Observation of microtremors and aftershocks of the 2016 Kumamoto earthquake in the Kumamoto basin

*Kosuke Chimoto[1], Hiroaki Yamanaka[1], Seiji Tsuno[2], Nobuyuki Yamada[3], Hiroe Miyake[4]

1. Tokyo Institute of Technology, 2. Railway Technical Research Institute, 3. University of Teacher Education Fukuoka, 4. The University of Tokyo

We have performed temporary strong motion observation for aftershocks of the 2016 Kumamoto earthquake at the damaged area due to the event (Yamanaka et al. 2016). We have already completed the observation in the town of Mashiki, village of Nishihara, city of Aso and village of Minamiaso, but the observation in the city of Kumamoto is still continued. We here report the strong motion records and microtremor measurements in the Kumamoto basin.

We have started the temporary strong motion observations immediately after the event of 17 April 2017. Several months after the observation, we removed and reinstalled the temporary stations in the city of Kumamoto and we here report the record observed mainly in July 2016. Two temporary stations were installed in Chuo-ward, one in Higashi-ward, three in Minami-ward, and two in Nishi-ward in the city of Kumamoto. The stations installed in Chuo-ward and Nishi-ward is close to the sites where the apartments had severe damage and liquefaction occurred. Less damage was found at the other stations. We used a seismometer JEP-6A3 (Mitutoyo Corp.) which has a sensitivity of 10V/G or 2V/G with a data logger LS7000XT or LS8800 (Hakusan Corp.). Stations continuously record ground motions with 100 Hz sampling and GPS signals were received for time correction.

It is observed 22 aftershocks with Mj 2~4. The strong motion records vary at each station. High frequency motions were observed at the stations located in the northern east of Kumamoto basin and in the Nishi-ward where the apartment was severely damaged. It is observed long period later phases at the stations in Minami-ward. It is also observed in the spectral ratio to the reference station in the northern east of the city of Kumamoto.

We conducted microtremor array measurements at all the temporary stations and estimated the shallow S-wave velocity structure. At any stations, the low velocity layer having a S-wave velocity of about 150m/s was found and its thickness was more than 15m. The thickness was more than 25m at the station in Minami-ward. It was about 2m at the station located in the middle terrace in Chuo-ward. The site response characteristics calculated from the shallow structures have the first dominant period at the period between about 0.5-1.0 seconds. It is more than 1 second at the station close to the coastline in Minami-ward.

This work was partly supported by the Grant-in-Aid for Special Purposes (16H06298: P.I. Hiroshi Shimizu).

Keywords: The 2016 Kumamoto earthquake, Temporary Strong Motion Observation, Aftershocks, Microtremors

Observation of aftershock due to the 2016 mid Tottori prefecture earthquake and microtremor observation in the structural damage area of mid Tottori prefecture, Japan

*Tatsuya Noguchi[1], Takao Kagawa[1], Shohei Yoshida[1], Sho Nakai[1], Hiroshi Ueno[1], Kazu Yoshimi[1], Shoya Arimura[1]

1. Department of Management of Social Systems and Civil Engineering, Civil Engineering Course Graduate School of Engineering, Tottori University

An earthquake (Mj6.6) occurred in central Tottori Prefecture in Japan on October 21, 2016. We conducted aftershock (strong motion) observation at several temporary sites in this area with housing damages. Characteristics of site amplification effect of the temporary sites were understood from analysis of seismic data. Also densely microtremor observations were carried out to estimate the characteristic of ground vibration in the damage area. Microtremor H/V spectra and a distribution of the predominant period were obtained from observation data. In addition, we checked the relationship between site effects and transfer functions of SH-wave, S-wave velocities, H/V of microtremor strong ground motion.

Keywords: 2016 mid Tottori Prefecture earthquake, aftershocks observation, microtremor observation

Site characteristics in Okayama prefecture inferred from strong-motion records of the 2016 Kumamoto earthquake

*Ayumu Uneoka[1], Masanao Komatsu[2], Hiroshi Takenaka[2], Keiichi Nishimura[3]

1. Okayama University, 2. Graduate school of Okayama University, 3. Okayama University of Science

The mainshock of the Kumamoto earthquakes (M_{JMA}7.3) occurred in Kumamoto prefecture, Japan, at 1:25 on 16 April 2016 (JST). The ground motion during this event observed on many stations in Southwest Japan, and several seismic stations in southern Okayama and a part of northern mountain area recorded a seismic intensity of 3 on the JMA scale. Since the azimuths, directions from the source toward the stations, are between 40-50 degrees in Okayama, we regard that the source and the path effects are not different for each station. Therefore, the difference among ground motions observed in Okayama only depends on the site effect under each station. In this study, we analyze strong-motion records in Okayama prefecture and evaluate the site characteristics under their stations. We use strong ground motion records at 113 stations from the networks of K-NET and KiK-net in NIED and seismic intensity meter in Okayama prefecture. We pick P- and S-wave arrivals and identify phases by polarization analysis. Since S-wave durations are for about 11 s from polarization analysis, we calculate Fourier spectra for 10 s after arriving S-wave. Setting on OKYH12 station (Ohara) built on the rock as a reference point, we calculate spectral ratio between another stations and the reference point. Also we compute H/V spectral ratio. Then, we measure primary peak frequency in each spectral ratio. Peak frequencies and shapes of spectral ratio for the reference point correspond to ones of H/V spectral raio in coast area and Hiruzen. However, in another area, primary peak frequencies of H/V are lower than ones of the ratio for reference point. Then, comparing to above peak frequency and site amplification rate in J-SHIS, seismic wave is well amplified under their stations, because 3320112 (Urayasu) and 3358860 (Tsuyama) stations have high site amplifications and low primary peak frequencies. Although 3321430 and 3358860 stations in Hiruzen have high PGA and PGV and low primary peak frequencies, site amplification rates are low. Hence, J-SHIS model cannot describe observed facts in their stations.
Acknowledgment: we used the strong-motions records of NIED and Okayama prefecture.

Keywords: Site characteristics, the 2016 Kumamoto earthquake, H/V spectral ratio

Estimation for site amplification characteristics from spectral inversion of ground motion records in Northern Nagano area

*kawai ryouta[1], Hiroaki Yamanaka[1], Kosuke Chimoto[1], Seiji Tsuno[2]

1. institute titech of tokyo, 2. Railway Technical Research Institute

The 2014 Northern Nagano Earthquake generated the maximum intensity of 6 lower at a strong motion station. The serious damage of this earthquake was characterized by a dense area which is 5km away from an observation station with an intensity of 5 higher. In this study we estimated site amplification characteristics by using ground motion records at strong motion stations and aftershock observation stations by Chimoto et al; (2016) in Northern Nagano area through a spectral inversion technique. The results of Q-value in the propagation path and source characteristics by the spectral inversion technique show similar to those from previous studies. The site amplification in a heavy damaged area show large values in a frequency range of 1.0-3.0[Hz]. A good correlation was found in the relationship between the amplification factors at low frequency and AVS30 from the previous studies, This suggest that the heavy damage is controlled by near-surface layers with low S-wave velocity

Keywords: Spectral inversion technique, Site amplification, 2014 Northern Nagano

A method for setting engineering bedrock using records of miniature array microtremor observation in Kanto Area

*Atsushi Wakai[1], Shigeki Senna[1], Kaoru Jin[1], Ikuo Cho[2], Hisanori Matsuyama[3], Hiroyuki Fujiwara[1]

1. National Research Institute for Earth Science and Disaster Resilience, 2. National Institute of Advanced Industrial Science and Technology, 3. OYO

1. Introduction
In order to estimate damage caused by strong ground motions from a mega-thrust earthquake, it is important to improve broadband ground-motion prediction accuracy in wide area. To realize it, it is one of the important challenges to sophisticate subsurface structure models.
On the purpose of precisely reproducing characteristics of seismic ground motions, we have ever collected as many data as possible obtained by boring surveys and microtremor array surveys, and then have modeled subsurface structure from seismic bedrock to ground surface. At present, we are modeling subsurface structure in Kanto and Tokai area in the project conducted by SIP (Cross-ministerial Strategic Innovation Promotion Program), “reinforcement of resilient disaster prevention and mitigation function” of Council for Science, Technology and innovation.
In this study, we attempt to sophisticate shallow subsurface structure models for Kanto area, including Tokyo, where miniature array microtremor surveys have been conducted from the second half of 2014 to 2016. The method is that initial geological models, which were developed based on boring data and surficial geological informaiton in the past, are improved using S-wave velocity structure estimated from records of miniature array microtremor observations. Especially, with connection between shallow and deep ground in mind, we will focus on boundary surface of velocity layer around engineering bedrock from Vs300 m/s to Vs500 m/s regarded as transitional range between shallow and deep ground.

2. Miniature array microtremor observation
About microtremor observations, array observations were conducted in lowland and plateau of Kanto area. It consists of 4-point miniature array with a radius of 60cm and 3-point irregular array from 3m to 10m on a side. These observations are made on the road and near seismic ground-motion stations such as K-NET and KiK-net. The total number of observation sites has reached about ten thousand, as of February in 2017. In addition, we made an observation for 15 minutes per site at intervals of 1km or 2km using JU210/215 or JU410 which is an all-in-one microtremor observation unit. Sampling frequency was 100Hz or 200Hz.

3. Analysis method and the results on shallow subsurface structure
In this study, we evaluated one-dimensional S-wave velocity structure using shallow subsurface structure survey method based on microtremor observation. The method has been proposed and advanced in recent researches [3-5]. We made an analysis in the following procedure using a microtremor analysis tool such as “BIDO” and “Microtremor Array Tools.”
[1]Auto-analysis and reading of disperse curves and H/V spectral ratios
[2]Extraction of amplification factors such as AVS30
[3]Direct depth transformation of disperse curves [Simple Profiling Method; SPM]
[4]Inversion process such as Simple Inversion Method [SIM]
[5]Joint inversion using H/V spectral ratio and initial velocity structure obtained in 3,4 noted above [Linear Inversion]
[6]Extraction of the depth of top surface in Vs350 m/s and Vs500 m/s layer

One-dimensional S-wave velocity structure and two-dimensional cross-section obtained by analysis mentioned above were, if necessary, modified after comparison with existing initial geological models and investigation. As a result, on the river basin, the models were consistent with S-wave velocity structure models based on boring data [initial geological models]. Besides, three-dimensional structure was revealed on velocity layers around engineering bedrock [Vs300 m/s to Vs500 m/s], which cannot be estimated only through boring data.

4. Summary

In this study, we estimated 1-D S-wave velocity structure and 2-D cross-section based on miniature array microtremor observation records in lowland and plateau of Kanto area. And then, more precisely, we set boundary surface of velocity layers after comparison with existing initial geological models and investigation. This challenge can be a key method about modeling of subsurface structure for seismic ground-motion prediction.

Keywords: engineering bedrock, S-wave velocity structure model, miniature array, microtremor

Modeling of 3D S-wave velocity structure for sedimentary layers in Kanto area, using microtremor array surveys –part 2-

*Kaoru Jin[1], Shigeki Senna[1], Atsushi Wakai[1], Hiroyuki Fujiwara[1]

1. National Research Institude for Earth Science and Disarster Prevention

We have ever engaged in modeling of underground structure from seismic bedrock to ground surface in Kanto area for the purpose of improving accuracy of earthquake ground-motion prediction. In order to advance the underground structure models, microtremor surveys have been conducted at a lot of sites in Kanto plain for these several years. “Senna et.al., 2016” shows that the conventional underground structure models were improved by using records of microtremor array surveys conducted by 2015 and earthquake observations.

In this study, by adding results of microtremor array surveys conducted at about 100 sites in 2016, the underground structure models were improved at the target area in comparison with models constructed in 2015. Above all, velocity layers from Vs500 m/s to Vs900 m/s were modified.

Keywords: microtremor array observation, S-wave velocity structure, Underground structure model

3D velocity structure of Oita prefecture, Kyushu, Japan for strong ground motion simulation

*Masayuki Yoshimi[1], Hisanori Matsuyama[2], Haruhiko Suzuki[2], Atsushi Yatagai[2], Takumi Hayashida[3], Shinichi Matsushima[4], Hiroshi Takenaka[5], Hiroe Miyake[6], Keiji Takemura[7]

1. Geological Survey of Japan, AIST, 2. Oyo Corporation, 3. Building Research Institute, 4. DPRI, Kyoto University, 5. Okayama University, 6. Tokyo University, 7. Kyoto University

For reliable strong ground motion prediction, valid velocity structure is essential. We constructed a 3D velocity structure of Oita prefecture up to engineering bedrock (Vs > 500 m/s) and finer 3d structure for Oita Plain additionally. In this study, we observed, collected, and compiled data obtained from microtremor surveys, ground motion observations, boreholes etc., and constructed velocity structure by modifying published one. Velocity structure up to the engineering bedrock is modified so as to reproduce the observed phase velocity and H/V ratio. Finer structure of the Oita Plain is modeled, as 250m-mesh model, with empirical relation among N-value, lithology, depth and Vs, using borehole data, then validated with the phase velocity data obtained by the dense microtremor array observation (Yoshimi et al., 2016).

This work is supported by the Comprehensive Research on the Beppu-Haneyama Fault Zone funded by the Ministry of Education, Culture, Sports, Science, and Technology (MEXT), Japan.

Keywords: shear wave velocity structure model, ground motion prediction, site amplification, microtremor observation

Evaluation of Three-dimensional Basin Structure Model beneath Beppu bay, Oita Prefecture, using Seismic Interferometry

*Takumi Hayashida[1], Masayuki Yoshimi[2], Masanao Komatsu[3], Hiroshi Takenaka[3]

1. IISEE, Building Research Institute, 2. Geological Survey of Japan, AIST, 3. Graduate School of Natural Science and Technology, Okayama University

A dense seismic array has been deployed since late August 2014 around the Beppu Bay area, Oita prefecture, Japan, to investigate S-wave velocity structure of deep sedimentary basin (Hayashida *et al.*, 2015; Yoshimi and Hayashida, 2017). The array consists of 12 stations with an average spacing of 12 km. Each station consists of a three component broadband seismometer (Nanometrics Trillium compact; 750 V/m/s, T=120 s) in a hole with a 24-bit data logger (Hakusan DATAMARK LS-8800; sampling rate of 100 Hz). We used the continuous ambient noise (microtremor) data of about 20 months (from September 2014 to April 2016) to obtain the ambient noise cross-correlation functions (CCFs) between 66 pairs of stations (6.4 km –65.2 km). The derived nine-component inter-station Green’s functions (ZR, ZT, ZZ, RR, RT, RZ, TR, TT, TZ) from the stacked cross-correlation functions show clear wave-trains corresponding to surface-wave propagation between sensors for station pairs that across shallow-bedrock areas, whereas it is still difficult to visually confirm the distinct wave trains for station pairs that across deep sedimentary basin beneath the Beppu Bay area. At first we investigated the spatial distribution of surface wave group velocities between two stations in different frequencies, by comparing the estimated group velocities from the derived CCFs with the multiple filtering technique (Dziewonski *et al.* 1969) and theoretical ones using an existing velocity structure model (J-SHIS v2). We also simulated theoretical Green’s functions for all stations pairs using the finite difference method (HOT-FDM, Nakamura et al., 2012), using the J-SHIS basin structure with land and seafloor topography and a seawater layer with a grid spacing of 50 m (Okunaka *et al.*, 2016). The estimated values of group velocity indicate smaller group velocities in the Beppu Bay area than those in the surrounding areas in the higher frequency range (0.3 Hz-) and generally show good agreements with theoretical ones. The comparisons between obtained and simulated Green’s functions also generally show good agreements in the areas in the frequency range between 0.1 and 0.5 Hz. On the other hand, the comparisons of group velocities and Green’s functions show systematic differences inside Beppu Bay, indicating S-wave velocity beneath the bay might be slower than those of the existing structure model.

Acknowledgements:
This work is supported by the Comprehensive Research on the Beppu-Haneyama Fault Zone funded by the Ministry of Education, Culture, Sports, Science, and Technology (MEXT), Japan.

Keywords: seismic interferometry, surface wave, group velocity, Green's function, ambient noise, finite difference method

The Estimation of 2D S-wave velocity structure model across the Morimoto-Togashi fault zone through miniature microtremor array analysis

*Nayuta Matsumoto[1], Yoshihiro Hiramatsu[2], Shigeki Senna[3]

1. Graduate School of Natural Science and Technology, Kanazawa University, 2. Institute of Science and Engineering, Kanazawa University, 3. National Research Institute for Earth Science and Disaster Resilience

Around the Noto peninsula, ENE-WSW or NE-SW striking reverse faults developed under the E-W compression stress in Quaternary (Okamura, 2007). It is important to reveal the subsurface structures of the faults, which have formed the topography of this region, to understand the geotectonic history of this area.
The object of our study is to reveal subsurface structures of the Morimoto-Togashi fault zone, which is located in southern part of the peninsula. The probability of a large earthquake occurring within the next 30 years is high, 2-8%, and the fault passes the city center of Kanazawa. Therefore, this study is also useful for the disaster prevention. A seismic reflection survey around Togiya, the north part of the Morimoto fault, suggests that the fault structure is an east dipping reverse fault with 40-60 degree, (AIST, 2008). However, the details of the subsurface structures are still unknown. Additionally, the gravity anomaly analysis cannot detect the structural boundary along the fault. In this study, we conduct miniature array analysis (Cho et al., 2013) using miniature arrays with a radius of 0.6 m and irregular-shaped arrays with a radius of 5-15 m. Sampling frequency is 200 Hz and the observation duration is around 15 minutes. Seismometers used for the observation are JU410 manufactured by Hakusan Corporation. We set 11 lines across the fault zone. The intervals of the observation points are 100-200 m. We analyze data with the software BIDO and infer the two-dimensional S-wave velocity sections. The software BIDO combines a simple profiling method (e.g., Heukelom and Foster, 1960), where an S-wave velocity structure is calculated directly from a dispersion curve, and a simplified inversion method (Pelekis and Athanasopoulos, 2011) to estimate the S-wave velocity structure. Around Togiya where the seismic reflection survey was held, the obtained S-wave velocity section shows a discontinuous structure of bedrock (Vs=500 m/s) on the 100 m east side of the surface fault trace. This discontinuity infers the east dipping structure with a high angle, corresponding to the faulting type of the fault.

Keywords: microtremor, miniature array, irregular-shaped array, velocity structure, active fault

Density Structure Model Estimated from Gravity Survey around Mashiki damaged by 2016 Kumamoto Earthquake

Shun Araki[2], Tatsuya Noguchi[3], Masao Komazawa[4], Shoya Arimura[3], Mitsuhiro Tamura[3], Kei Nakayama[3], *Hitoshi Morikawa[1], Takashi Miyamoto[5], Kahori Iiyama[1], Yoshiya Hata[6], Masayuki Yoshimi[7], Takao Kagawa[3], Hiroyuki Goto[8]

1. Department of Urban Design and Built Environemt, Tokyo Institute of Technology, 2. Department of Civil and Environmental Engineering, Tokyo Institute of Technology, 3. Department of Management Social Systems and Civil Engineering, Tottori University, 4. Oyo Corporation, 5. Department of Civil Engineering, Yamanashi Univsersity, 6. Division of Global Architecture, Osaka University, 7. Geological Survey of Japan, AIST, 8. Disaster Prevention Research Institute, Kyoto University

Gravity survey has been carried out around downtown of Mashiki, Kumamoto, Japan, where is severely damaged by 2016 Kumamoto earthquake, from November 28 to December 2, 2016. We applied three LaCoste gravimeters and one Schintrex CG-3M. Closed observations were carried out at more than 300 sites around the central part of Mashiki with about 50-meter intervals. And, more than 150 sites surround the central part with 250- to 500-meter intervals. The observation sites satisfy enough density to discuss density structure shallower than 500-meter depth around central part of Mashiki. After applying some corrections to the observed data, the Bouguer anomaly is calculated under the assumed density of 2.4 g/cm^3. Furthermore, gravity basement is estimated under an assumption of two layered medium with density difference of 0.5 g/cm^3. As a result, a graben runs parallel to the Akitsu river and some isolated small basins are found inside of the graben. The central part of Mashiki is located immediately above of the one of such the small basins. This may suggest that the focusing phenomena of seismic rays.

Keywords: Gravity Survey, Mashiki, Kumamoto, Japan, Density Structure

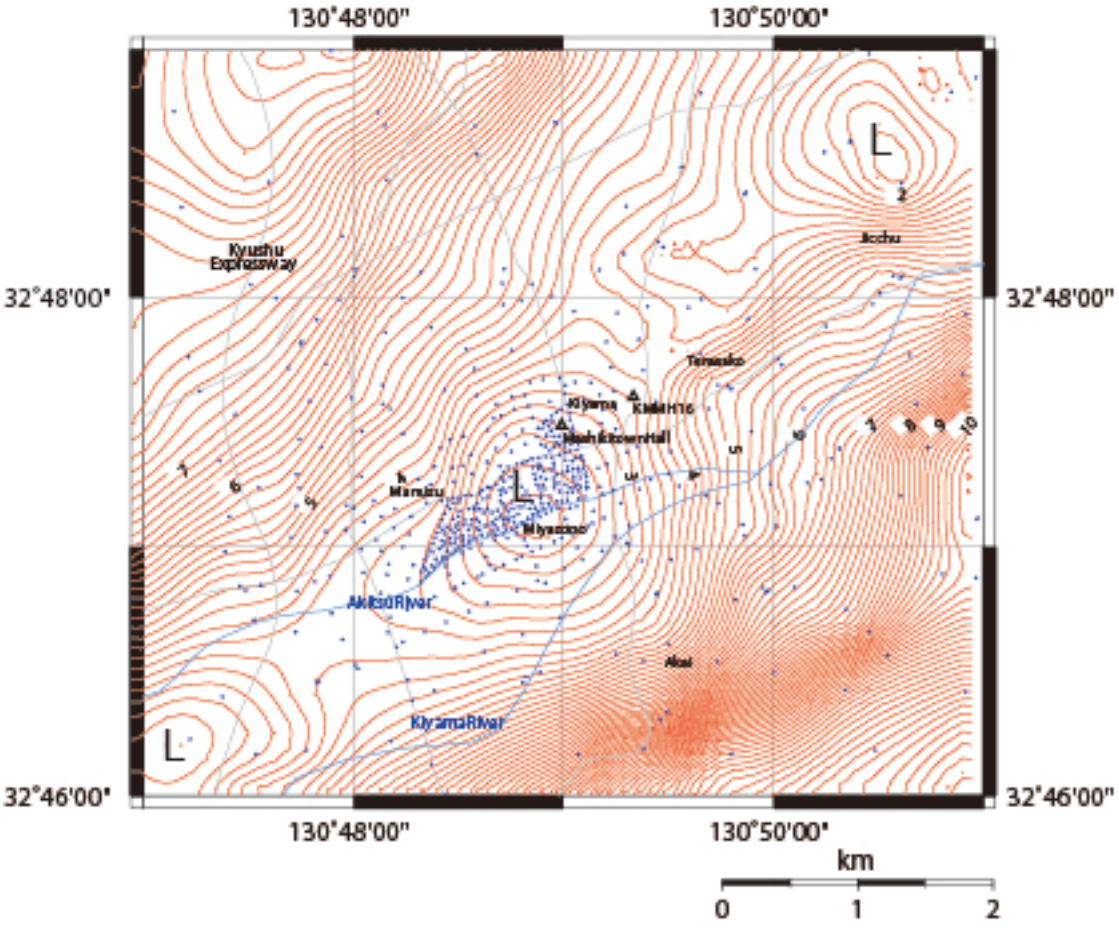

Bouruer anomaly (assumed density = 2.4 g/cm³)

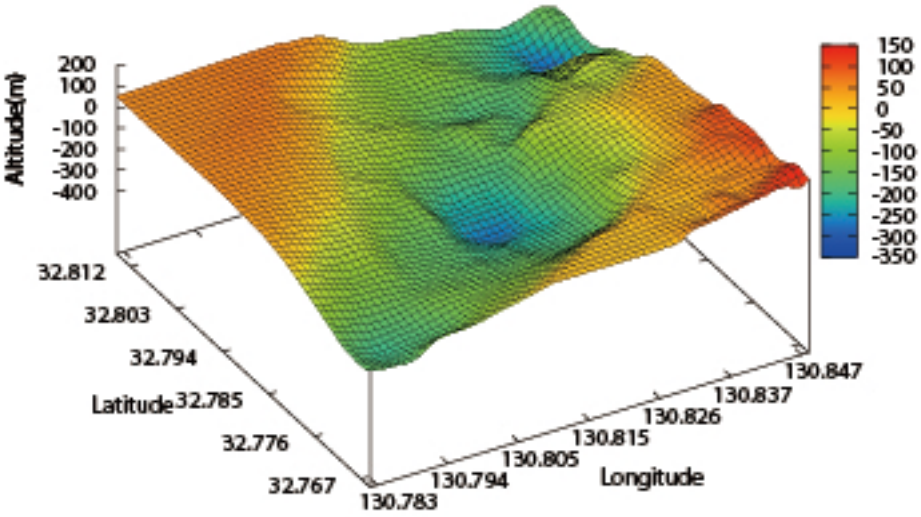

Gravity basement (density difference = 0.5 g/cm³)

Microtremor Array Measurement Survey and Strong Ground Motion Observation Activities of the SATREPS, MarDiM Project, Turkey

*seckin ozgur citak[1], Safa Arslan[2], Ozlem Karagoz[3,7], Kosuke Chimoto[3], Oguz Ozel[2], Hiroaki Yamanaka[3], Bengi Aksahin[2], Ken Hatayama[4], Michihiro Ohori[5], Muneo Hori[6]

1. Japan Agency for Marine-Earth Science and Technology (JAMSTEC), Research and Development Center for Earthquake and Tsunami (CEAT), Yokohama, Japan, 2. Istanbul University, Department of Geophysical Engineering, Istanbul, Turkey, 3. Tokyo Institute of Technology, Dept of Environmental Science and Technology, Yokohama, Japan, 4. National Research Institute of Fire and Disaster, Tokyo, Japan, 5. Fukui University, Research Institute of Nuclear Engineering, Fukui, Japan, 6. University of Tokyo, Earthquake Research Institute, Tokyo, Japan, 7. Canakkale Onsekiz Mart University, Department of Geophysical Engineering, Canakkale, Turkey

Since 1939, devastating earthquakes with magnitude greater than seven ruptured North Anatolian Fault (NAF) westward, starting from 1939 Erzincan (Ms=7.9) at the eastern Turkey and including the latest 1999 Izmit-Golcuk (Ms=7.4) and the Duzce (Ms=7.2) earthquakes in the eastern Marmara region, Turkey. On the other hand, the west of the Sea of Marmara an Mw7.4 earthquake ruptured the NAF’ s Ganos segment in 1912. The only un-ruptured segments of the NAF in the last century are within the Sea of Marmara, and are identified as a "seismic gap" zone that its rupture may cause a devastating earthquake. In order to unravel the seismic risks of the Marmara region a comprehensive multidisciplinary research project The MarDiM project "Earthquake And Tsunami Disaster Mitigation in The Marmara Region and Disaster Education in Turkey", has already been started since 2003. The project is conducted in the framework of “Science and Technology Research Partnership for Sustainable Development (SATREPS)” sponsored by Japan Science and Technology Agency (JST) and Japan International Cooperation Agency (JICA).

One of the main research field of the project is "Seismic characterization and damage prediction" which aims to improve the prediction accuracy of the estimation of the damages induced by strong ground motions and tsunamis based on reliable source parameters, detailed deep and shallow velocity structure and building data. As for detailed deep and shallow velocity structure microtremor array measurement surveys were conducted in Zeytinburnu district of Istanbul, Tekirdag, Canakkale and Edirne provinces at about 140 sites on October 2013, September 2014, 2015 and 2016. Also in September 2014, 11 accelerometer units were installed mainly in public buildings in both Zeytinburnu and Tekirdag area and are currently in operation. Each accelerometer unit compose of a Network Sensor (CV-374A) by Tokyo Sokushin, post processing PC for data storage and power supply unit. The Network Sensor (CV-374A) consist of three servo type accelerometers for two horizontal and one vertical component combined with 24 bit AD converter.

In the presentation current achievements and activities of research group, preliminary results of microtremor array measurement surveys and recorded data by the newly installed stations will be introduced.

Keywords: Satreps, MarDiM project, Seismic observation, Microtremor array measurement

Elaboration of a velocity model of the Bogota basin (Colombia) based on microtremors array and gravity measurements, and strong motion records

*Nelson Pulido[1], Shigeki Senna[1], Hiroaki Yamanaka[2], Helber Garcia[3], Leonardo Quiñones[4], Chimoto Kosuke[2], Cristina Dimaté[4], Mario Leal[5]

1. National Research Institute for Earth Science and Disaster Resilience, 2. Tokyo Institute of Technology, 3. Servicio Geológico Colombiano (Colombian Geological Survey), 4. Universidad Nacional de Colombia (National University of Colombia), 5. Instituto Distrital de Gestión de Riesgos y Cambio Climático (Bogota Agency for Risk Management and Climatic Change)

Bogotá, a megacity with almost 8 million inhabitants is prone to a significant earthquake hazard due to nearby active faults as well as subduction megathrust earthquakes. The city has been severely affected by many historical earthquakes in the last 500 years, reaching MM intensities of 8 or more in Bogotá. The city is also located at a large lacustrine basin composed of extremely soft soils which may strongly amplify the ground shaking from earthquakes. The basin extends approximately 40 km from North to South, is bounded by the Andes range to the East and South, and sharply deepens towards the West of Bogotá. The city has been the subject of multiple microzonations studies which have contributed to gain a good knowledge on the geotechnical zonation of the city and tectonic setting of the region. To improve our knowledge on the seismic risk of the city as one of the topics, we started a 5 years project sponsored by SATREPS (a joint program of JICA and JST), entitled “Application of state of the art technologies to strengthen research and response to seismic, volcanic and tsunami events and enhance risk management in Colombia (2015-2019)”. In this paper we will show our preliminary results for the elaboration of a velocity model of the city. To construct a velocity model of the basin we conducted multi-sized microtremors arrays measurements (radius from 60 cm up to 1000 m) at 41 sites within the city. We calculated dispersion curves and inferred velocity profiles at all the sites. We combine these results with available gravity measurements within the city to obtain the initial velocity model of the basin. We also evaluated site effects in Bogota using records from the Strong Motion Network of Bogota.

Keywords: Site Effects, Strong motion, Bogota basin, microtremors array, gravity

Observation of source rupture directivity and site effect using earthquake early warning systems

*Ting-Yu Hsu[1], Pei-Yang Lin[2], Hung-Wei Chiang[2], Shieh-Kung Huang[2]

1. Taiwan TECH & NCREE, 2. NCREE

The National Center for Research on Earthquake Engineering (NCREE) in Taiwan has developed an on-site Earthquake Early Warning System (NEEWS). The Meinong earthquake with a moment magnitude of 6.53 and a focal depth of 14.6 km occurred on February 5, 2016 in southern Taiwan. It caused 117 deaths, injured 551, caused the collapse of six buildings, and serious damage to 247 buildings. During the Meinong earthquake, the system performance of sixteen NEEWS stations was recorded. The directivity of the earthquake source characteristic and also possibly the site effects were observed in the diagram of the distribution of PGA difference between the predicted PGA and the measured PGA. In addition, based on a preassigned PGA threshold to issue alarms at different stations, no false alarms or missed alarms were issued during the earthquake. About 4 seconds to 33 seconds of lead-time were provided by the NEEWS depending on the epicenter distance.

Keywords: Source Rupture Directivity, Site Effect, On-Site Earthquake Early Warning

Multi-use seismic stations for earthquake early warning

Stephen Kilty[1], Bruce Townsend[1], Geoffrey Bainbridge[1], David Easton[1], *Nahanni McIntosh[1]

1. Nanometrics Seismic Monitoring Solutions

Earthquake Early Warning (EEW) network performance improves with the number and density of sensing stations, quality of the sites and of strong-motion instrumentation, degree of coverage near at-risk populated areas and potential fault zones, and minimizing latency of signal processing and transmission. Seismic research tends to emphasize competing requirements: low-noise sites, high-performance broadband seismic instrumentation, and high-quality signal processing without regard for latency. Recent advances in instrumentation and processing techniques have made feasible the concept of a multi-use seismic station in which strong- and weak-motion seismometry are both cost-effectively served without compromising the performance demands of either.

Our concept for a multi-use seismic station meets the needs of both EEW and high-quality seismic research. One significant enabler is a 6-channel dual-sensor instrument that combines a 120s broadband seismometer and a class A accelerometer in a single ultra-compact sonde suitable for direct burial. Combining two sensors effectively adds broadband capability to a station without increasing the already optimized site footprint, preparation and management costs associated with shallow direct-burial installations. The combined sensors also simplify and speed up installation (for example, the accelerometer provides real-time tilt readings useful to leveling the seismometer). Integration simplifies alignment to north, as there is only one instrument to orient. A dual-use 6-channel digitizer simultaneously provides two sets of independently processed streams from both sensors, one set optimized for low-latency earthquake warning, and the other set for high-quality seismic research purposes.

Such a dual-use seismic station can serve both seismic research and civil warning infrastructure objectives without adding significantly to the cost of a single-use station, while increasing the utility for all users of the station’ s data.

Keywords: earthquake early warning, broadband seismometer, accelerometer, multi-use seismic station

Development of inference methods for rotational motions on ground surface

*koji hada[1], Horike Masanori [2]

1. NEWJEC INC., 2. Hanshin Consultants Co., Ltd.

In this study, we develop two methods for the inference of rotation vector on ground surface, two rocking rotations and a single torsional rotation. The first, termed nth-order elastic method, is based on the elasticity of the ground surface, and the rotation vector is constructed from the first derivative of ground motions which are approximated by nth-order Taylor expansion. Meanwhile, the second, termed rigid method, is based on the rigidity of ground surface and the rotation vectors are directly obtained by the least square method which minimize the sum of the squared difference between recorded differential motions and the equation of the rigid motions. Furthermore, the second is divided into two methods. The one, multi-site rigid method, uses the differential motions at multi sites, while the other, single-site rigid method, uses the differential motions at a single site. Also, we show that the 1st-order elastic method is the same as the rigid method. Appling the nth-order elastic method to microtremor recordings acquired with a small-size dense array, we successfully infer the rotation vector and find the rigid zone with a radius of 5m for the torsional motions. We furthermore obtain the two findings. The first is that the rotation vector can be inferred with a simpler array of a small size and a fewer observation sites. The second is that the root mean squared (RMS) amplitudes of the torsional rotation inferred by the single site rigid method are approximately the same as the RMS amplitudes obtained by the 1st-order elastic method in a zone close to the reference site.

Keywords: Inference methods of rotational motions, Ground surface, Microtremors, Small-size dense array

Study on the backtracking factors of Arias Intensity based on the Ground-motion response spectrum and time-period envelope function parameters

*Liang Xiao[1]

1. Institude of Geophysics, China Earthquake Administration

Arias intensity, as a parameter descripting ground motion amplitude and duration characteristics, has good correlation with earthquake damage such as landslide and sand soil liquefaction. The study on the relationship between the Arias Intensity and the ground-motion response spectrum has important application value in the rapid assessment of earthquake disaster, seismic landslide hazard analysis and so on.
Our previous research found it was difficult to backtrack or reproduce Arias Intensity by using only response spectrum through artificial ground-motion. *Ts*, a critical parameter of the envelope function, defined as the duration of stationary portion of an earthquake record, was found to have great influence on the backtracking results of the artificial Arias Intensity. However, *Ts* could vary a lot due to different rules of definition. Thus, one proper definition of *Ts* is needed to meet the demand for backtracking of Arias Intensity.
In this paper, a set of strong ground-motion records chosen from U.S. PEER NGA database were used as the basic data. The corresponding response spectrum (5% damping ratio) and Arias Intensity was calculated. *Ts* for each record were calculated using several frequently-used definitions. Artificial ground-motion acceleration time periods were generated and were used to reproduce artificial Arias Intensity.
The statistical difference between real values of Arias Intensity and artificial ones were identified. The proper *Ts* was defined as the one that minimizes the difference between the statistical mean of artificial Arias Intensity and the real values. Additional tests showed that backtracking of Arias Intensity could be improved in a statistical sense by using both the response spectrum and proper *Ts* parameter.

Keywords: Arias Intensity, Strong ground-motion, Response spectrum

The detailed explanation of the strong resemblance between Fourier Spectrum and Phase difference Spectrum of the Seismic Wave.(Science of Form)

*Masaru Nishizawa[1]

1. none

1.The phase difference Spectrum and The Phase Wave of the seismic wave.
Fig-(1). Show “The relationship between the phase difference spectrum and the phase wave”. Please refer to reference (3). Find the phase difference Spectrum from the phase wave on the right -hand side, the peak position and added an expanse state of Spectrum are in perfect harmony accord. In short (in other words), in case of the frequency of the phase wave is high, the shape of the normal distribution of the phase difference spectrum is build up sharp. And in the case of large frequency get a flat normal distribution of spectrum. This phenomena stand up all right frequency is high or low. Of course this phenomena is reversible was stated reference (3).
I shall state a next item 2, the seismic wave and this phase wave should be a one-to-one relation. And still more the Fourier spectrum of the seismic wave and the phase difference Spectrum should be a one-to-one relation.
2.The Fourier Spectrum and the normal distribution of seismic wave.
We think that the case of the epicenter length is becoming shorter little by little. The large epicenter length to get along with, the seismic wave energy is dispersed in every direction and still more had died out. As a result, the shape of the Fourier spectrum don’t become a hill shape and happened occasionally a pointed shape. The shorter epicenter length to get along with, the shape of the Fourier spectrum of seismic wave is formed a hill and soon are considered the shape of the normal distribution.
Reference. “Earthquake” written by Seismologist KIYOO Wadachi. The Chuukou Library. (A pocket edition) 1933 and 1993(reprint) p.99
“In the near area to the epicenter, the earthquake have very sharp motion. In many case, intense vertical motion happens in the early shocks of an earthquake. The longer the epicenter length little by little, vibration of seismic wave become slow little by little and becomes superior in a horizontal vibration.”
The shape of this normal distribution has flat hill and besides has large frequency of the peak of the hill. But get shorter little by little, the shape of the normal distribution (or Bell type) becomes sharp and becomes short frequency.
Moreover make the short epicenter length, we shall study the normal distribution theory (Gaussian distribution, Mt.Fuji-type or Bell type) of probability and statics.
In the reference (4), I have explained the KdV equation.(literature (3),(4))
Abstract
1. The shorter epicenter length shorter, the shape of the normal distribution becomes sharp. And this frequency too becomes small. The case of the epicenter length is large, the normal distribution of spectrum of seismic wave was not build up. Only build up a scattered peak.
2. On the case of the phase wave and the phase difference spectrum, the same phenomenon too come into being.
Reference
1. Yorihiko Osaki "Shin Jishindou no Spectrum Kaiseki Nyumon" P78.
2. Masaru NISHIZAWA. (2012): Study of shape of Mountain (Normal Distribution) of Fourier Spectrum of Earthquake Motion. May 20-25, S-SS30-P12(2012, JpGU)

3. Masaru NISHIZAWA. (2012): Handling by Solitary Wave and soliton of Earthquake Motion: October D22-01, 2012, The Seismological Society of Japan.
4. Masaru NISHIZAWA. (2015): Normal Distribution of Seismic Wave Spectrum and Solitary Wave in Water Waves (Science of Form). October 27. S01-P20, 2015, The Seismological Society of Japan.
5. Research Report on the 2011 Great East Japan Earthquake Disaster. NIED, Japan.

* Reference 1: The very excellent and the easy to understand book. I can say with confidence.

Keywords: Fourier Spectrum, Phase difference spectrum, Seismic wave, Phase wave, KdV equation, Solitary wave

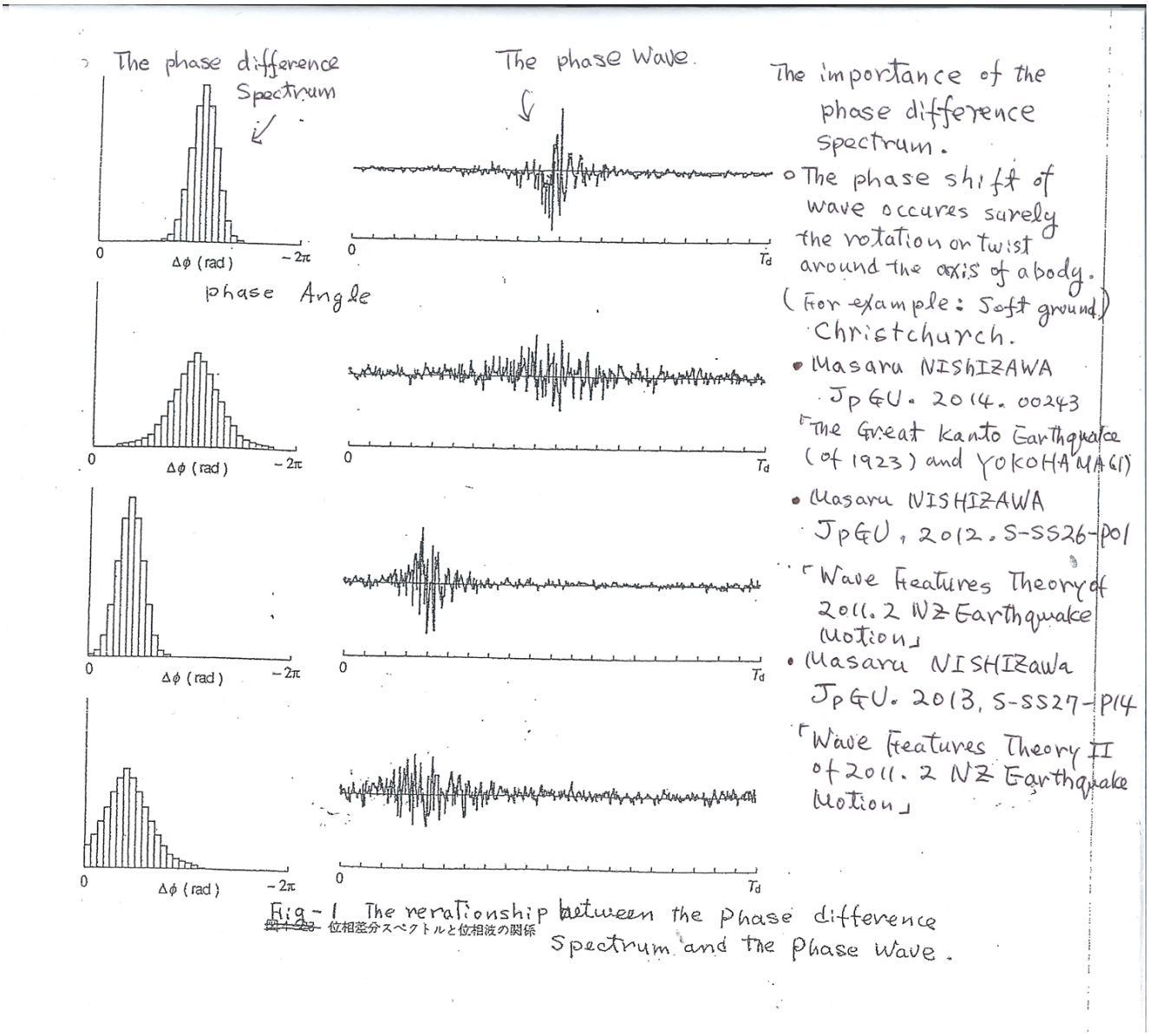

Fig-1 The neralionship between the phase difference Spectrum and the phase wave.
位相差分スペクトルと位相波の関係

